ornl

OAK RIDGE NATIONAL LABORATORY

LOCKHEED MARTIN

MANAGED AND OPERATED BY
LOCKHEED MARTIN ENERGY RESEARCH CORPORATION
FOR THE UNITED STATES
DEPARTMENT OF ENERGY

ORNL-27 (3-96)

ORNL/TM-13450

R-Matrix Analysis of the ^{240}Pu Neutron Cross Sections in the Thermal to 5700 eV Energy Range

H. Derrien
O. Bouland
N. M. Larson
L. C. Leal

ORNL/TM-13450

R-MATRIX ANALYSIS OF THE ^{240}Pu NEUTRON CROSS SECTIONS IN THE THERMAL TO 5700 eV ENERGY RANGE

H. Derrien
Nuclear Energy Agency Data Bank, OECD, Paris (France)

O. Bouland
Centre d'Etudes, Cadarache, Commissariat Energie Atomique (France)

N. M. Larson and L. C. Leal
Oak Ridge National Laboratory, Oak Ridge, Tennessee (USA)

Date Published: August 1997

Prepared by the
Oak Ridge National Laboratory
Oak Ridge, Tennessee 37831-2008
Managed by
LOCKHEED MARTIN ENERGY RESEARCH CORP.
for the
U.S. DEPARTMENT OF ENERGY
under contract DE-AC05-96OR22464

Table of Contents

ABSTRACT

Resonance analysis of high resolution neutron transmission data and of fission cross sections were performed in the neutron energy range from the thermal region to 5700 eV by using the Reich-Moore Bayesian code SAMMY. The experimental data base is described and the method of analysis is given. The experimental data were carefully examined in order to identify more resonances than those found in the current evaluated data files. The statistical properties of the resonance parameters are given. A new set of the average values of the parameters is proposed, which could be used for calculation of the average cross sections in the unresolved resonance region. The resonance parameters are available in ENDF-6 format at the national or international data centers.

INTRODUCTION

The neutron cross-sections of ^{240}Pu were re-examined both at thermal energy and in the resolved resonance region, in order to eliminate the discrepancies revealed by the JEF-2 validation studies.[1] The results of this re-evaluation are compared with data from ENDF/B-VI, JEF-2 and JENDL-3. The evaluations of the resonance parameters of these files were principally based on the work of Kolar et al.[2] who analyzed high resolution transmission measurements in order to obtain the energies and the neutron widths of the resonances in the energy range from 20 eV to 5700 eV, and on the results of Weston et al.[3] who obtained the fission widths from high resolution measurements of the fission cross-section in the same energy range. The parameters of the resonance at 1.056 eV, which accounts for more than 90% of the capture resonance integral, were due to Spencer et al.,[4] except in the JENDL-3 file, where older values were used.

As much information as possible was adopted from the available experimental data and analyzed using the SAMMY[5] resonance analysis code which allows a correlated sequential fit of the experimental data. The first section of this paper gives a general description of the analysis. The experimental data base is described in Section II. In Section III, the results of the analysis are reviewed and compared with the data in the current files. In Section IV, the properties of the resonance parameters are examined.

I. GENERAL DESCRIPTION OF THE ANALYSIS

The computer code SAMMY uses the Reich-Moore approximation to the R matrix formalism[6] for calculation of cross-sections in the resonance region. The calculated cross sections are fitted to the experimental data by solving Bayes equations for the variable parameter values. The analysis of a set of experimental data provides the values for the physical parameters pertaining to the formalism, the adjustable experimental parameters (background corrections, normalization, sample temperature etc.) and the covariance matrix corresponding to those parameters. These parameters and their covariance matrix can then be used as input to SAMMY for analyzing another set of experimental data. The inclusion of experimental parameters ensures the consistency of a data base containing several independent sets of experimental data. If the changes in the experimental parameters of a set of data are too large, one could suspect the corresponding measurement and remove it from the data base.

The Reich-Moore formalism is most useful for the analysis of the cross sections of fissile nuclei because it can account for strong interferences between resonances in the fission channels. The multi-level Breit-Wigner formalism could be appropriate for the description of the ^{240}Pu cross section, since the fission induced by neutrons in the resonances of ^{240}Pu is a subthreshold fission and the fission widths are usually small. However, one fundamental aspect of the fission cross-section of ^{240}Pu is the presence of an intermediate structure due to the coupling between the class I states (resonances) and the class II states of the second well of the double-humped fission barrier. In the vicinity of the class II states (clusters of fission resonances), the fission widths of the resonances could be large enough to create non-negligible interference effects. It is therefore important to use a more accurate formalism, such as Reich-Moore. The Reich-Moore formalism

had already been used by Auchampaugh et al.[7] for the description of the cross-sections in the fission clusters. The nature of the interferences (constructive or destructive) depends on the relative sign of the fission width amplitudes. Usually the sign is determined from the shape of large interference effects. It is clear that the interferences in the fission cross section of ^{240}Pu are imperceptible in the resonances located between the class II states. Therefore, at the beginning of the analysis, the sign of the fission widths must be assigned randomly, which also makes it possible to avoid an unrealistic accumulation of weak effects in the same direction. Some relative signs can be determined in the fission clusters, with good probability, from the shape of the fission cross-section.

In general, the best experimental data for the identification of resonances are thick sample transmission data having good statistical accuracy. Very small resonances located between the largest resonances can be detected in this way. The transmission data available for the evaluation of ^{240}Pu were obtained from relatively thin samples with rather poor counting statistics; neither the authors of the measurements nor the evaluators made any attempt to identify the small resonances in the high energy part of the experimental data. In the present work, the transmission measurements were carefully examined so as to identify a larger number of small resonances up to a neutron energy of 5700 eV.

Before starting the analysis over an extended energy range, it is necessary to calculate the contribution of the negative energy resonances and of the resonances beyond the upper limit of the energy region being analyzed (the so-called external resonances). These contributions could be obtained with good accuracy by using the resonance parameters of ENDF/B-VI. The method involves applying an energy shift to all the ENDF/B-VI resonances to bring them into the negative region and applying another energy shift to bring them into the higher energy region. The contributions, in the energy range to be analyzed, of this sample of external resonances can then be calculated by using the SAMMY code with the two shifted sets of resonances. This calculated contribution could be directly introduced into file 3 of the ENDF-6 format. However, it is preferable to simulate the contributions with a limited number of resonances (four at negative energies and four in the higher region, in the present case) whose parameters are obtained using the SAMMY code to fit the calculated contributions. The results obtained for the total cross section of ^{240}Pu are shown in Figure 1. It will be assumed that the contributions of the more remote resonances, and of resonances of angular momentum greater than 0, are smaller than the experimental error in the data analyzed, and, therefore, negligible. In particular, the value R of the effective scattering radius should remain constant throughout the energy range analyzed. However the samples used in the transmission measurements were too thin to give a satisfactory accuracy for the potential scattering cross section. The value of R=9.42 fm used in the present work is that which was obtained for ^{239}Pu by Derrien.[8]

II. DESCRIPTION OF THE EXPERIMENTAL DATA BASE

The most recent experimental data in the thermal region and over the 1.056 eV resonance are the results of the transmission measurements performed by Harvey et al.[9] and Spencer et al.[4] Accurate values of the total cross section at 0.0253 eV and of the parameters of the 1.056 eV

resonance were obtained by Spencer et al., but their experimental transmission data were not available for the present evaluation. The transmission results of Harvey et al. were obtained using samples containing 99% of ^{239}Pu and only 1% of ^{240}Pu, which nevertheless permit analysis of the ^{240}Pu resonance at 1.056 eV. These data were not analyzed by the authors but were available for the present evaluation.

Most of the other experimental data available at low energy are very old and of little use for an accurate evaluation of the parameters of the resonance at 1.056 eV, owing to a lack of information on the experimental conditions. However, the total cross-section obtained by Block et al.[10] can be used for the determination of the shape of the cross-section in the energy range from 0.02 eV to 0.15 eV. The measurements at low energy of the fission cross-section performed by Leonard et al.[11] are the only ones available for the evaluation of the fission width of the resonance at 1.056 eV. Besides the precise values for the total and absorption cross-sections at 0.0253 eV obtained by Spencer et al., the values obtained by Block et al., Pattenden et al.[12], Tattersall et al.,[13] Halperin et al.[14] and Lounsbury et al.[15] were also considered.

In the energy range up to 5700 eV, transmission measurements and fission cross-section measurements were available. The transmission measurements were performed by Kolar et al.[2] for three samples of thicknesses, 0.000513 at/barn, 0.00166 at/barn, and 0.00416 at/barn, respectively. Only the total cross-sections obtained from the two thickest samples were published. Information about the experimental errors is vague, but had to be used to reconstruct the statistical errors on each measured point. The measurements were performed in the energy range from 20 eV to 700 eV for the medium sample and in the energy range from 20 eV to 5700 eV for the thickest sample. To facilitate the analysis by SAMMY, the total cross-sections were converted back to transmissions. Preliminary calculations using the ENDF/B-VI resonance parameters showed that substantial corrections for normalization and background were needed to the transmission data of the thick sample in the lower energy range. The correction parameters were obtained from preliminary SAMMY fits in a few selected energy ranges. They are given in Table 1. Other preliminary fits were performed on major isolated resonances in order to obtain precise values for the parameters of the experimental resolution, particularly the contribution of the neutron moderator and of the exponential tail of the resolution function. The results are given in Table 2.

The fission cross-section in the region of resolved resonances has been measured by several authors: Byers et al.,[16] Migneco et al.,[17] Weigmann et al.,[18] Auchampaugh et al.[7] and Weston et al.[3], mainly for determining the parameters of the class II states and of the double-humped fission barrier. Only the measurements by Weston and Auchampaugh have the qualities of resolution and experimental statistics needed for the determination of the fission widths of a large number of class I states. A set of fission widths was obtained by Auchampaugh from a Breit-Wigner analysis of the resonances located in the energy ranges between the class II states and a Reich-Moore analysis of the resonances in the fission clusters. Unfortunately, the experimental fission cross-sections used in the analysis were not published. In the present work only the fission cross-section measurements of Weston were analyzed.

There are no high resolution measurements of the capture cross-section in the resonance region. The only available results are those of Weston et al.[19] obtained from measurements of

average cross-sections between 200 eV and 350 keV. These average values are compared with those calculated from the resonance parameters.

Most of the experimental data were obtained by the neutron time-of-flight technique using an electron linear accelerator to provide a pulsed neutron source, or a neutron chopper on a neutron beam from a reactor. The accuracy of the determination of the neutron energy of a time-of-flight spectrum depends on the accurate knowledge of the neutron path length and of the time of flight of the neutrons. Before analyzing all the experimental data, each experiment must be calibrated by means of a selected experiment in order to obtain a consistent energy scale. In general the most precise energy is given by the longest flight path. One of the transmission measurements of Kolar et al. was selected for the energy scale determination, since these measurements were performed with a 100 m flight path. The deviation D(E) between two energy scales corresponding to two different time-of-flight experiments is given by the following equation:

$$D(E) = aE + bE^{3/2}$$

where the coefficient a is related to the error on the length L of the flight path and b to the error on the neutron flight time *t*. The energy E (eV), the flight time t (μs) and the length L (m) of the flight path are related as follows:

$$E = (72.3L)^2/t^2$$

The coefficients a and b could be determined by measuring the energy difference for two well-defined resonances. But, in general, the deviation D(E) is evaluated over a large number of resonances and the coefficients a and b are then obtained by a least-square fit to the linear plot of D(E)/E as a function of $E^{1/2}$. It was not necessary to align the fission cross-section measurements of Weston on the transmission measurements of Kolar, since this was already done by the authors of the evaluation for ENDF/B-VI.[20] On the other hand, the medium sample transmission measurements of Kolar had to be aligned on the thick sample measurements. A few adjustments had to be made also for the low energy measurements of the resonance at 1.056 eV.

III. THE RESULTS OF THE ANALYSIS

For the Doppler broadening of the resonances, an effective temperature of 296 K was used for all the experiments carried out at room temperature except for the analysis of the 1.056 eV resonance for which the temperature proposed by Spencer was adopted.

A. The thermal cross-sections and the parameters of the resonance at 1.056 eV

The absorption cross-section at 0.0253 eV obtained by Lounsbury with a quoted high accuracy is not consistent with the value obtained by Spencer. The value obtained by Lounsbury is 289.5±1.4 b which compares with the value of 282 ± 3 b obtained by Spencer from the measurement of the total cross section and an estimated value of 2 b for the elastic scattering cross-

section. The result of Lounsbury was a by-product of the measurement of the ratio of the capture cross-section to the fission cross-section, and of the measurement of the fission cross-sections of ^{233}U, ^{235}U and ^{239}Pu. The error quoted by Lounsbury could be under-estimated compared with the more direct measurement of Spencer. It is also possible to infer the total cross-section at 0.0253 eV from the measurements of Block in the energy range from 0.020 eV to 0.15 eV. One obtains a value of 290±8 b which is not in contradiction (in view of the large uncertainty) with the value of 284±2 b proposed by Spencer.

A SAMMY analysis was performed in the energy range from 0.020 eV to 1.50 eV. The experimental data base included the total cross-section data of Block between 0.020 eV and 0.15 eV, the transmission data of Harvey between 0.20 eV and 1.5 eV (two sample thicknesses) and the fission cross-section measurements of Leonard between 0.30 eV and 1.3 eV. The input resonance parameters used in the SAMMY calculation include the fictitious external resonances, the resonances between 0 eV and 5700 eV, and the ^{239}Pu resonances in ENDF/B-VI needed for the exact representation of the transmission measurements of Harvey. The calculated cross-sections were fitted to the experimental data by varying the parameters of one negative energy resonance and the resonance at 1.056 eV. The cross-sections calculated at 0.0253 eV were as follows:

total	288.5	b
scattering	2.7	b
fission	0.059	b
absorption	285.7	b

The total cross-section at 0.0253 eV is a compromise between the ENDF/B-VI value and that of Spencer. The parameters of the resonance at 1.056 eV are given in Table 3. They differ very little from those of Spencer. The results of the SAMMY fits are shown on Figures 2 and 3.

B. Energy range from 19 eV to 5700 eV

The analysis was performed in the energy range 19 eV to 5700 eV using an experimental data base including the transmission data of Kolar and the fission cross section measurements of Weston. Between 19 eV and 700 eV the SAMMY fits were performed sequentially in the following order: medium sample transmission, thick sample transmission, fission cross-sections. Above the energy of 700 eV only the transmission data obtained using the thick sample were available together with the fission cross sections. A few examples of graphical comparisons between the experimental data and the corresponding data calculated from the resonance parameters obtained from the SAMMY fits are shown in Figures 4 to 10. The thick sample transmission data were first corrected for background and normalization obtained in the preliminary analyses. During the final fits, the background and the normalization parameters were still variable, but gave only small corrections which were within the values of the experimental errors.

The average values of the capture cross-section, calculated from the pointwise data generated from the resonance parameters using NJOY, are given in Table 4 and are compared with the values calculated from ENDF/B-VI, JEF-2 and JENDL-3 and with the experimental values of Weston. In the energy range from 0.02 eV to 200 eV, where there are no experimental capture data, all the evaluations agree within 2%. In the energy range from 200 eV to 5000 eV, the JEF-2 and JENDL-3 evaluations were probably normalized to the average value of Weston. The average value of ENDF/B-VI is 27% below that of Weston, which means that, in the evaluation for ENDF/B-VI, Weston disregarded his own experimental values. No comment was made by Weston on this point. The results of the present evaluation agree with ENDF/B-VI. They are, on the average, 25% below the values of JEF-2. The average values of the fission cross section are given in Table 5. The values of ENDF/B-VI, JENDL-3 and of the present evaluation are similar. They are in good agreement with the experimental data of Weston analyzed in the present work. The values of JEF-2 are about four times higher in the energy range from 1 eV to 800 eV.

The capture and fission resonance integrals are equal to 8481 b and 3.16 b, respectively, compared with the values of 8494 b and 2.46 b of ENDF/B-VI, 8445 b and 3.52 b of JEF-2, and 8102 b and 2.29 b of JENDL-3. With regard to capture, the JENDL-3 value is 5% lower than the others; this is due mainly to the fact that in JENDL-3 the neutron width of the resonance at 1.056 eV is 7% lower than the value in the other evaluations.

The resonance parameters are given in the Appendix of this report. The number of resonances in the energy range from 0 eV to 5700 eV is 425. In ENDF/B-VI, only 267 resonances were represented in the same energy interval, more precisely 22% less in the energy range from 0 to 1.5 keV and 44% less in the energy range from 1.5 keV to 5.7 keV. The 158 resonances which have been added to the new file have been identified by a careful examination of the experimental fission cross-section and transmission data.

The experimental fission cross-section data of Weston were used to identify resonances which do not appear in the transmission data of Kolar, especially below 2 keV where the experimental resolution of Weston measurements is excellent. These resonances do not show up in the experimental transmission data if their neutron width is too small. They do not emerge above the potential scattering cross section and the large statistical fluctuations of the experimental transmission data. But they could be seen above a residual fission cross-section which is very close to zero. Authors of previous evaluations have not attempted to explain the presence of these resonances in the fission cross-section and simply retained only the resonances identified by Kolar. Figure 11 shows a typical example of this situation. Only the four large resonances identified by Kolar were used to represent the fission data. It is clear that three additional resonances, at energies 1.529 keV, 1.555 keV and 1.582 keV, should be added. The resonances at 1.529 keV and 1.582 keV have neutron widths of 5 meV and 3 meV, respectively, and are just observable in the statistical fluctuations of the transmission data; the resonance at 1.555 eV has a neutron width of about 2.5 meV and is not visible in the transmission data.

By a careful observation of the experimental transmission data it was also possible to identify other small resonances in the statistical fluctuations of the data, especially above 1.5 keV. Some of these resonances are obvious; others are probable. A typical example is given in Figure 12 in the energy range from 3.250 keV to 3.375 keV where 10 resonances should be identified, against only 2 in ENDF/B-VI. The reduced neutron widths of these resonances are smaller than 0.25

meV, i.e., 20% of the average value. The eight additional resonances give a reasonable average spacing of 12.0 eV in this energy interval.

IV. STATISTICAL PROPERTIES OF THE RESONANCE PARAMETERS

The study of the statistical properties of the resonance parameters is needed for the evaluation of the average parameters used for the cross section calculations in the region of unresolved resonances and for the evaluation of the optical model parameters used for the cross section calculations at higher energy. Consideration of the statistical properties makes it possible to verify the consistency of the parameters obtained in the analysis of the experimental data. All the resonances were regarded as belonging to s wave neutrons, i.e., to a single population of spin 1/2. The ratio of the penetration factors of s- and p-waves is equal to about 0.005 at a neutron energy of 1 keV and to 0.02 at a neutron energy of 5 keV. Some small resonances might therefore be p-wave resonances. However, the existing experimental data do not allow the distinction between the smallest s-wave resonances and large p-wave resonances. The confusion between the small s-wave resonances and the p-wave resonances should compensate to some extent for a shortage of detected small s-wave resonances and hence should not perturb the observed properties of the s-wave resonances.

A. The average resonance spacing and the Wigner distribution

The number of resonances identified in the energy interval from 0 eV to an energy of E eV is shown as a function of the energy E in Figure 13. The plot shows a linear behavior up to an energy of 2750 eV, with an average spacing of 12.06 eV. Above 2750 eV the average spacing is 16.10 eV, showing a 25% loss of resonances compared with the lower energy region. There is still a substantial lack of small resonances in the high energy region. This is due mainly to the rapid increase in the width of the resolution function which has the effect of increasingly flattening the small resonances, causing them to disappear into the statistical fluctuations of the transmission. No resonance with a reduced neutron width smaller than 0.045 meV was identified in the energy range from 2750 eV to 5700 eV, while 40 resonances of this type were identified at energies below 2750 eV. These 40 resonances would be sufficient to restore the average spacing to about 12 eV over the entire energy range analyzed. One must conclude, therefore, that the sample of resonances which has most chance of being representative of ^{240}Pu is that consisting of the resonances identified in the energy range from 0 eV to 2750 eV.

The distribution of the spacings of resonances pertaining to a single spin state should obey the Wigner law. The experimental differential distribution of the resonance spacings in the energy range from 0 eV to 2750 eV is given in Figure 14, with the Wigner distribution normalized to the total number of spacings. There is a good agreement between the experimental histogram and the theoretical law.

B. The reduced neutron widths, the strength function and the Porter-Thomas distribution

The variation, as a function of the energy E, of the sum from 0 to E of the reduced neutron widths $\Gamma_n^0 = \Gamma_n / \sqrt{E}$ is shown in Figure 15. This variation should be linear with a slope equal to the strength function $s_0 = \left(\sum_0^E \Gamma_n^0\right)/E$. Three slopes are observed in the experimental histogram, corresponding to the strength function 1.069×10^{-4} between 0 eV and 2800 eV; 0.696×10^{-4} between 2800 eV and 3900 eV, and 1.158×10^{-4} between 3900 eV and 5700 eV. The second value is statistically incompatible with the others and might suggest a non-statistical effect in the entrance channel of the interaction of the s-wave neutron with the ^{240}Pu nucleus. The local values of the strength function in energy intervals of 500 eV are also shown in Table 6. The sampling error $(2/N)^{1/2}$ is equal to about 22% in each interval. The values of 0.731×10^{-4} and 0.661×10^{-4} observed in the energy intervals 3 keV to 3.5 keV and 3.5 keV to 4.0 keV respectively are in fact incompatible with the other values. Such abnormal values of the local strength functions were also observed by Olsen et al.[21] for ^{238}U, which is a nucleus similar to ^{240}Pu. Table 6 shows also the values calculated from ENDF/B-VI. There is an agreement within 2% at low energy. Above 2 keV, the ENDF/B-VI values are 16% lower on the average. This difference is due mainly to the large number of resonances which were added to the file in the present work. In the evaluation for ENDF/B-VI, Weston added a smooth background in file 3 of the evaluation in order to compensate for the effect of unidentified resonances. This smooth background is not needed in the present evaluation since the very small resonances which are still missing at high energy contribute less than 0.2% to the strength function (about 40 resonances with an average reduced neutron width smaller than 0.02 meV).

The reduced neutron widths should be distributed according to the Porter-Thomas law, i.e., a chi-square distribution with one degree of freedom. The differential distribution of the reduced neutron widths for the resonances in the energy range from 0 eV to 2750 eV is represented by the histogram in Figure 16, where the experimental distribution is compared with the Porter-Thomas law. There is good agreement between the experimental and the theoretical distributions. However, one notes an unexpectedly high number of values of Γ_n^0 around 0.1 meV. This could be due to the resonances which were more or less guessed in the statistical fluctuations of the transmission data and for which the neutron widths were probably overestimated, and also to the resonances that appear only in fission and which were attributed a value of Γ_n^0 corresponding to the detection threshold of small resonances in the transmission data. Some of these resonances might also be induced by the p-wave neutrons.

C. The fission widths

The compound nucleus, (^{240}Pu + neutron), undergoes fission through a barrier which is about 1 MeV above the neutron binding energy. This subthreshold fission shows an intermediate structure in the fission cross section due to the coupling between the class I states (resonances) and the class II states of the second well of the double-humped fission barrier. The properties of this intermediate structure has been investigated by several authors[7, 17, 18] in order to determine the properties of the fission barrier and of the class II states. The fission cross-section is enhanced in

the resonances in the vicinity of the class II states. These resonances constitute what is known as fission clusters. About 22 fission clusters have been observed in the energy range below 10 keV, giving an average spacing of the class II states of about 450 eV.[18] The parameters of the intermediate structure were not obtained in the present work, since the fission cross sections in the fission clusters could be calculated by SAMMY from the parameters of the resonances well resolved in all the clusters in the energy range investigated.

The average values of the fission widths of the resonances located in the energy ranges between the fission clusters are given in Table 7 and compared with the values calculated from ENDF/B-VI. These values characterize the direct penetration of the two fission barriers. The average value of all these fission widths is 0.68 meV, which compares with 0.44 meV for ENDF/B-VI. The fission widths are much higher in the fission clusters. The largest values are given in Table 8 together with those obtained by Auchampaugh and by Weston. Auchampaugh interpreted the resonance doublet at 1402.4 eV and 1408.5 eV as an example of degeneracy between an unperturbed class I state and an unperturbed class II state, according to the theoretical studies of Lynn,[22] and Bjornholm and Lynn.[23] However, the fission width he obtained for the resonance at 1408.5 eV is much larger than that obtained in the present work and by Weston. That might cast doubt on the results obtained by Auchampaugh on the coupling parameters of the class I states and the class II states. The fission widths obtained in the present work in the fission clusters are in general in good agreement with the values proposed by Weston except for the resonance doublet at 2692.9 eV and 2696.4 eV, which was not resolved in Weston's data nor in those of Auchampaugh.

In general, the fission widths of the resonances are distributed according to a chi-square distribution in which the number of degrees of freedom is related to the number of open or partially open fission channels. In the case of the fission induced by neutrons on ^{240}Pu, the presence of the intermediate structure prevents a conventional statistical treatment of the fission widths. The parameters of the structures should be determined by directly investigating the experimental fission cross-sections in an energy range extending up to a few hundreds of keV. This was not the purpose of the present work.

D. Radiative capture widths

The radiative capture width Γ_γ was obtained for 78 prominent resonances in the energy range from 0 to 2 keV. For the small resonances below 2 keV and for all the resonances above 2 keV, the capture width was kept constant in the SAMMY fits at a value very close to the average value. The statistical error on Γ_γ obtained by the SAMMY fits was about 3% at low energy and about 10% towards 2 keV. The average values in 250 eV energy intervals are given in Table 9. The average value in the energy range from 0 eV to 2 keV is 31.92 meV with a statistical error of 0.34 meV and a systematic error of about 1.50 meV. This value is 4% higher than the average value of 30.6 meV used in ENDF/B-VI. The fluctuations of the radiative capture widths from resonance to resonance should theoretically be small since the number of channels in the capture process is very high. The large fluctuations of 20 to 25% observed in the present results are mainly due to the experimental and the analysis errors.

E. Recommended average values of the s-wave resonance parameters.

The average values are the following:

	Present results	BNL[24]
Resonance spacing	12.06 ± 0.60 eV	13.6 ± 0.7 eV
Strength Function	$(1.032 \pm 0.071)\times10^{-4}$	$(0.93 \pm 0.08)\times10^{-4}$
Capture Width	31.92 ± 1.60 meV	31 ± 2 meV

The average resonance spacing is that obtained in the energy interval from 0 eV to 2750 eV where the resonance parameters have the expected statistical properties. The strength function is obtained in the energy ranges from 0 eV to 5700 eV; the effect on the strength function of resonances not identified in the high energy regions is negligible, since these resonances have very small reduced neutron widths.

V. CONCLUSIONS

A new set of resonance parameters suitable for the representation of the neutron cross-sections of ^{240}Pu in the energy range from 0 eV to 5700 eV has been obtained by a consistent SAMMY analysis of experimental transmission and fission data of high resolution. A special effort was made to identify the small resonances in the transmission and fission data. A much more comprehensive set of resonances has been obtained. The resonance parameters were obtained with improved accuracy by using a method of analysis much more efficient than the method used in older work. However, the parameters of the resonance at 1.056 eV differ very little from the accurate values obtained by Spencer et al., also from a SAMMY analysis of experimental transmission data. The resonance capture integral is changed very little when compared with JEF-2 and ENDF/B-VI , since more than 90% of it is due to the first resonance.

In the energy range from 200 eV to 5000 eV, the average capture cross section is 27% lower than the values of JEF-2 and JENDL-3. The average experimental values of Weston, which were used as a basis for the JEF-2 and JENDL-3 evaluations, should be renormalized. This renormalization should also result in the revision of the evaluated data files at energies above 5700 eV. The average values of the fission cross section are in good agreement with ENDF/B-VI, JENDL-3 and with the experimental data of Weston. However, the average fission cross-section of JEF-2 is about 4 times too high in the energy range from 1 eV to 800 eV.

VI. ACKNOWLEDGEMENT

This work was supported by the Nuclear Energy Agency of OECD (Paris, France) and by Electrecite De France (EDF, France). Part of the work was performed at Oak Ridge National Laboratory with the technical assistance of the ORELA staff. The help of J. Harvey and D. Larson is particularly acknowledged.

VII. REFERENCES

1. E. Fort and M. Salvatores, "JEF-2 Validation Methodology, Present results, Future plans", pp.768-73 in *International Conference on Nuclear Data for Science and Technology, Gatlinburg, Tennessee, May 9-13, 1994.*

2. W. Kolar and K. H. Bockhoff, *Nucl. Energy*, **22**, 299 (1968).

3. L. W. Weston and J. H. Todd, *Nucl. Sci. Eng.* **88**, 567 (1984).

4. R. Spencer et al., *Nucl. Sci. Eng.*, **96**, 318 (1986).

5. N. M. Larson, *User's Guide for SAMMY: Multilevel R-matrix Fits to Neutron Data Using Bayes' Equations*, Oak Ridge National Laboratory report ORNL/TM-9179 (August 1984), ORNL/TM-9179/R1 (July 1985), ORNL/TM-9179/R2 (June 1989), and ORNL/TM-9179/R3 (Sept 1996).

6. C. W. Reich and M. S. Moore, *Phys. Rev.*, **111**, 929 (1958).

7. G. F. Auchampaugh and L. W. Weston, *Phys. Rev,* **C12**, 1850 (1975).

8. H. Derrien, J. *Nucl. Sci. Tech.*, **30**(9), 845 (1993).

9. J. H. Harvey et al., Private communication.

10. R. C. Block et al., *Nucl. Sci. Eng.*, **8**, 112 (1960).

11. B. R. Leonard et al., *Bull. Am. Phys. Soc.* **1**: 248 (June 1956).

12. N. S. Pattenden and V. S. Rainy, *J. Nucl. Energy, Part A*, Vol. 11, 14 (1959).

13. Tattersall, *J. Nucl. Energy, Part A*, Vol. **12**, 32 (1960).

14. J. Halperin et al., *J. Inorg. & Nucl. Chem.*, **9** (1), 1 (1959).

15. M. Lounsbury et al., *Proc. Int. Conf. Nuclear Data for Reactors*, Helsinki, June 15-19, 1970, Vol. I, p.287, IAEA Vienna (1970).

16. D. H. Byers, *Conf. on Neutron Cross Section Technology, Washington, March 1966*, Vol. 2, p. 903 (1966).

17. E. Migneco and J. P. Theobald, *Nucl. Phys.*, **A112**, 603 (1968).

18. H. Weigmann et al., *Nucl. Phys.*, **A187**, 305 (1972).

19. L. W. Weston and J. H. Todd, Nucl. Sci. Eng., **63**, 143 (1977).

20. L. W. Weston, *Evaluation of the Neutron Cross Sections for Pu-240,* ORNL/TM-10386; ENDF-343 (1988).

21. D. K. Olsen et al., *Nucl. Sci .Eng.*, **94**, 102 (1986).

22. E. Lynn, *The Theory of Neutron Resonance Reactions*, Clarendon, Oxford (1968).

23. S. Bjornholm and J. E .Lynn, *Rev. Mod. Phy.* **52**, 4, 725 (1980).

24. S. F. Mughabghab, *Neutron Cross Sections*, Vol. 1, Part B, Academic Press, Inc. (1984).

Table 1. Renormalization coefficients and residual backgrounds obtained in preliminary SAMMY analyses of the thick sample transmission measurements Kolar et al.[a]

Energy[b] (eV)	Normalization	Background
20	0.770	0.0330
38	0.880	0.0246
70	0.921	0.0157
90	0.938	0.0097
97	0.944	0.0099
152	0.958	0.0090
287	0.963	0.0104
566	0.969	0.0081
805	0.977	0.0085
1190	0.976	0.0104
1560	0.983	0.0081
1770	0.984	0.0081
2230	0.976	0.0103
2640	0.982	0.0082
4100	0.977	0.0102

[a] W. Kolar and K. H. Bockhoff, *Nucl. Energy*, 22, 299 (1968).
[b]Average energy of the range where the adjustments were performed.

Table 2. Results of the adjustment of the resolution parameters from a preliminary SAMMY analysis of isolated resonances *in the* transmission measurements of Kolar et al.[a] Δ L corresponds to the uncertainty on the length of the flight path due mainly to the slowing down of the neutrons in the moderator. Δ Texp is the parameter of the exponential tail of the resolution function, as defined in SAMMY.[b]

Energy[c] (eV)	ΔL (cm)	ΔTexp (ns)
66.8	3.39	24.5
92.0	3.69	29.0
28.0	3.73	29.1
56.0	3.13	26.9
81.0	3.12	29.5
1190.0	3.26	25.7
1570.0	3.21	24.0
1650.0	3.23	22.4
1770.0	3.18	24.3
2280.0	3.21	24.4
2640.0	3.25	25.2

[a] W. Kolar and K. H. Bockhoff, *Nucl. Energy*, 22, 299 (1968).
[b] N. M. Larson, *User's Guide for SAMMY: Multilevel R-matrix Fits to Neutron Data Using Bayes' Equations*, Oak Ridge National Laboratory report ORNL/TM-9179 (August 1984), ORNL/TM-9179/R1 (July 1985), ORNL/TM-9179/R2 (June 1989), and ORNL/TM-9179/R3 (Sept 1996).
[c]Average energy of the range where the adjustments were performed. The average values of Δ L = 3.31 cm and of ΔTexp=25.91 were used in the final SAMMY fits.

Table 3. Parameters of the resonance at 1.056 eV.

	This work	Spencer et al[a]
E eV	1.0564	1.0564
Γ_n meV	2.45 ± 0.02	2.45 ± 0.02
Γ_γ meV	29.15 ± 0.06	30.3 ± 0.3
Γ_f meV	0.0081 ± 0.0015	

[a] R. Spencer et al., *Nucl. Sci. Eng.*, **96**, 318 (1986).

Table 4. Average values of the capture cross-sections calculated using NJOY. The values obtained in the present work are compared with those obtained from other evaluated data files, and with the experimental values of Weston et al.[a]

Energy range (eV)	Weston	Capture cross sections (b)			
		This work	ENDF/B-VI	JEF-2	JENDL
0.02-1.5		5922	5930	5897	5652
1.5-50		56.85	56.83	55.34	57.33
50-100		49.96	44.04	48.57	48.71
100-200		23.30	26.40	25.57	25.64
200-300	8.71±0.61	7.27	7.41	9.07	9.08
300-400	10.27±0.72	7.93	7.89	9.92	9.94
400-500	6.60±0.46	6.01	5.97	7.02	7.03
500-600	7.14±0.50	6.22	5.91	7.15	7.16
600-700	5.09±0.36	4.44	4.64	4.65	4.65
700-800	2.63±0.18	2.04	1.64	3.31	3.31
800-900	6.63±0.46	5.70	5.25	5.31	5.31
900-1000	5.53±0.39	5.75	5.47	6.15	6.15
1000-1500	3.50±0.25	3.13	2.89	3.46	3.46
1500-2000	3.03±0.21	2.52	2.24	3.05	3.05
2000-3000	2.42±0.17	1.90	1.54	2.40	2.40
3000-4000	1.89±0.13	1.20	1.29	1.89	1.90
4000-5000	1.67±0.12	1.13	1.55	1.76	1.75
5000-5700		0.95	1.54	1.60	1.60
0.02-200		81.76	82.09	81.99	80.73
200-5000	3.02	2.42	2.37	3.03	3.03

[a]L. W. Weston and J. H. Todd, Nucl. Sci. Eng., **63**, 143 (1977).

Table 5. Average values of the fission cross-sections calculated using NJOY. The values obtained in the present work are compared with those obtained from other evaluated data files.

Energy range (eV)	This work	Fission cross sections (mb)		
		ENDF/B-VI	JEF-2	JENDL
0.02-1.5	1649	1170	1140	1048
1.5-50	91	94	381	94
50-100	74	76	346	76
100-200	46	50	337	50
200-300	52	53	222	53
300-400	15	1.8	228	18
400-500	47	49	188	49
500-600	20	23	185	21
600-700	54	54	208	66
700-800	879	905	1020	938
800-900	698	615	693	613
900-1000	86	80	155	75
1000-1500	206	199	257	147
1500-2000	316	297	422	312
2000-3000	210	181	332	242
3000-4000	75	74	116	6
4000-5000	60	50	88	67
5000-5700	150	145	91	124
1.5-5700	159.5	148.7	227.9	157.6
The JENDL average value between 1.5 eV and 5700 eV takes into account the correction of the abnormal value of the energy range 3000 eV to 4000 eV.				

Table 6. Local values of the strength function obtained in the present work compared with those calculated from ENDF/B-VI. Large differences are observed above 1.5 keV, due mainly to a significant number of missing resonances in ENDF/B-VI .

Energy range (eV)	This work		ENDF/B-VI	
	Strength Function × 10^4	Number of resonances	Strength Function × 10^4	Number of resonances
0-500	1.089	42	1.102(- 1.2%)	36
1500-2000	1.221	39	1.167(+4.6%)	26
2000-2500	0.993	40	0. 9 I I (+9. 0%)	25
2500-3000	1.041	36	0.948(+9.8%)	21
3000-3500	0.731	37	0.628(+16 %)	17
3500-4000	0.661	34	0.539(+23 %)	16
4000-4500	1.215	35	0.952(+28 %)	18
4500-5000	1.032	31	0.896(+15 %)	18
500-1000	1.049	42	1.027(+2.1%)	33
1000-1500	1.021	45	1.008(+I.3%)	32
5000-5700	1.206	44	1.047(+15 %)	25
The relative deviations between this work and ENDF/B-VI are given in brackets.				

Table 7. Average fission widths of the resonances between the class II states. The differences between the present values and those obtained from ENDF/B-VI could be due to the larger number of resonances identified in the present work.

Energy range (eV)	(Γ_f) meV	
	ENDF/B-VI	This work
0-720	0.18(47)	0.18(58)
1000-1300	0.96(17)	1.83(26)
1500-1800	0.54(14)	0.90(24)
2100-2500	0.30(20)	0.32(32)
2800-3000	0.61(11)	0.53(12)
3500-3900	0.72(11)	0.65(28)
4000-4400	0.43(15)	1.16(28)
The number of resonances in each sample is given in brackets.		

Table 8. Fission widths of the resonances in the fission clusters. One notes large differences at 1408 eV and 2693 eV with the Auchampaugh et al.[a] and the Weston et al.[b] results.

Resonance energy (eV)	This work (meV)	Auchampaugh[a] (meV)	Weston[b] (meV)	Γ_n^0 (mev)
782.44	1859±36	1450±400	1486±40	0.14
993.00	8000±2000			0.01
1402.44	2086±61	2000±200	2139±68	0.260
1408.50	85±3	1500±200	86±1000	0.260
1937.00	1810±156	2200±600		0.045
2692.93	111±1	164±18	1313±41	6.280
2696.40	58±4			0.290
3382	2265±169		3923±249	0.270

[a] G. F. Auchampaugh and L. W. Weston, *Phys. Rev,* **C12**, 1850 (1975).
[b] L. W. Weston and J. H. Todd, *Nucl. Sci. Eng.* **88**, 567 (1984).

Table 9. Average values of the radiative capture widths in energy intervals of 250 eV. The average value of all the 78 values obtained in the SAMMY fits is 31.9 meV.

Energy range (eV)	$\langle\Gamma_\gamma\rangle$ (meV)	Absolute error (meV)	
		Statistical	Systematic
0-250	30.0(13)	0.8	0.7
250-500	34.4(11)	0.9	0.8
500-750	33.2(13)	0.8	0.7
750-1000	31.8(14)	0.8	0.7
1000-1250	31.3(10)	1.0	1.0
1250-1500	31.1(5)	1.3	1.7
1500-1750	31.6(6)	1.2	1.5
1750-2000	31.1(6)	1.2	1.5

The number of resonances in each sample is given in brackets.

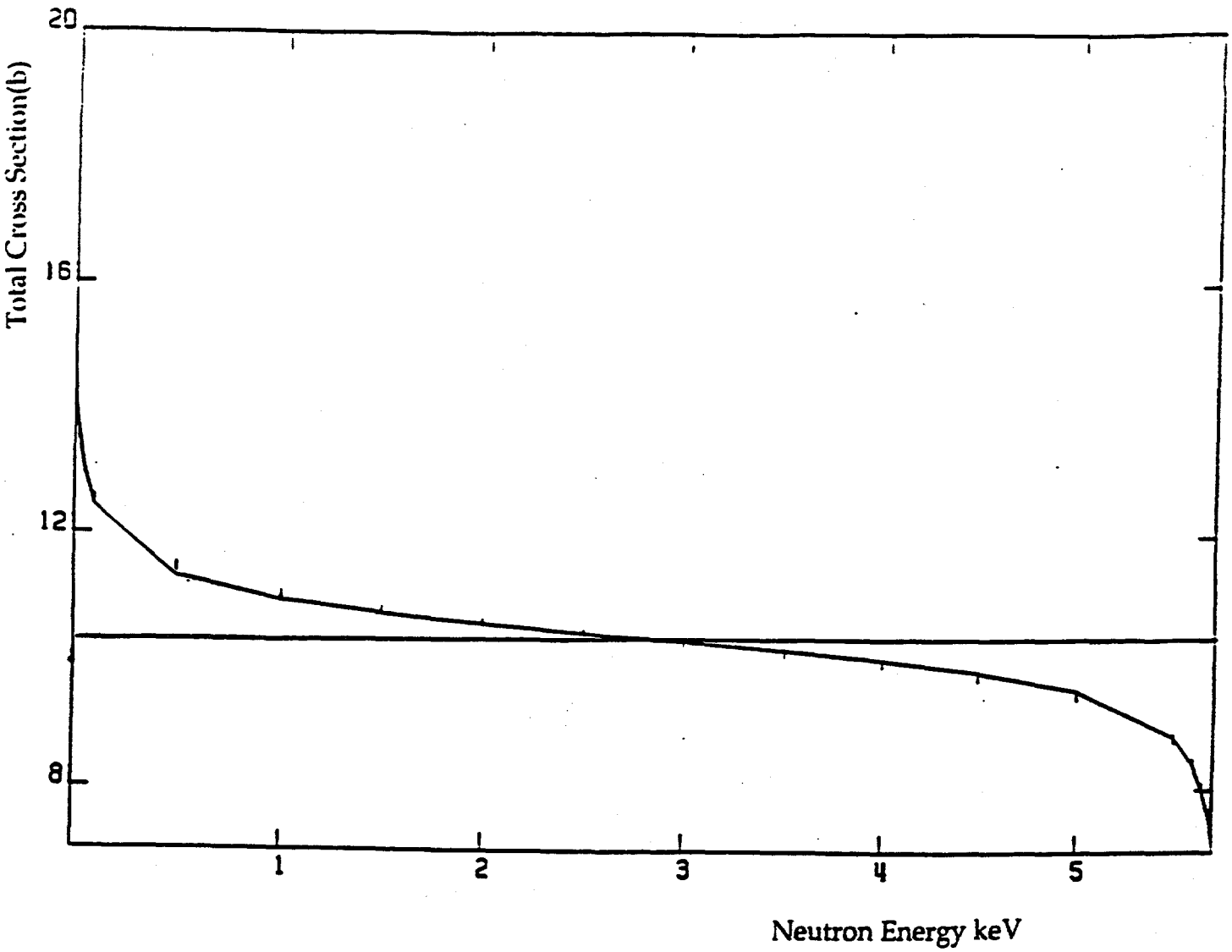

Figure 1- Contribution of external resonances to the total cross section in the energy range from 0 eV to 5700 eV. The vertical lines represent the cross sections calculated by a complete set of external resonance parameters. The solid line is the result of a SAMMY fit with only 4 fictitious negative energy resonances and 4 fictitious resonances at energies above 5700 eV.

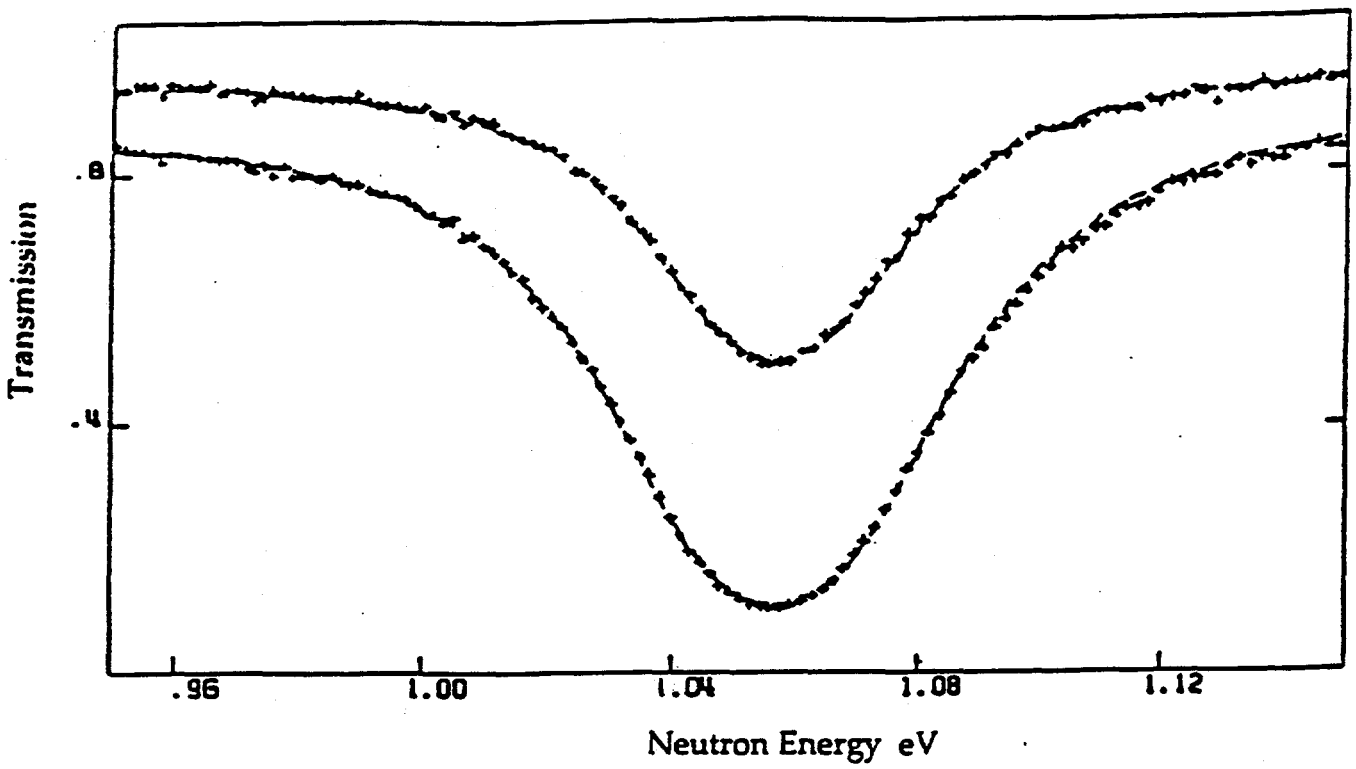

Figure 2- Transmission data in the resonance at 1.056 eV (two sample thicknesses). The crosses are the results of the measurements by Harvey et al.[9] The dotted curves were calculated with the resonance parameters.

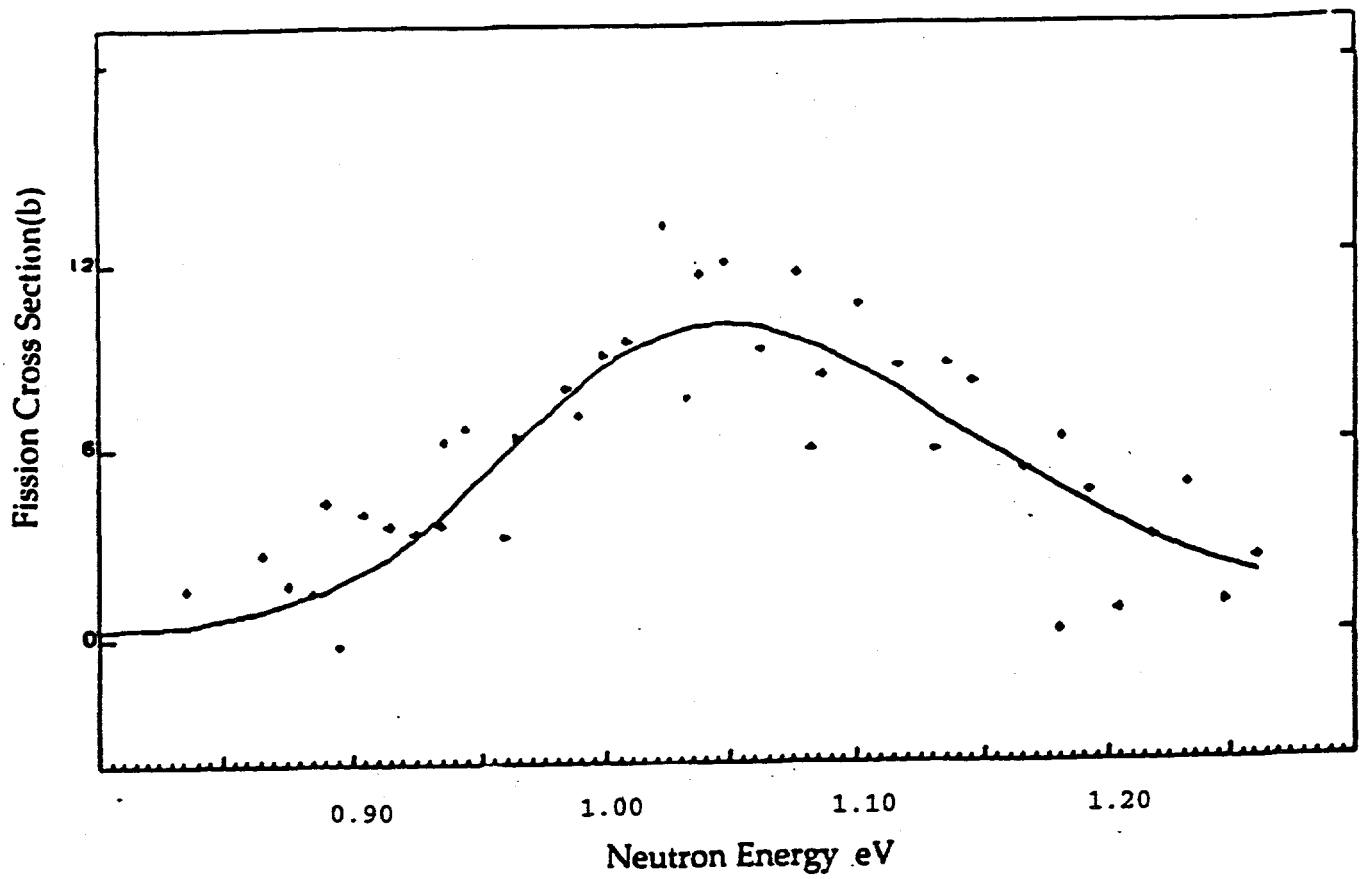

Figure 3- The fission cross-section of the resonance at 1.056 eV.The crosses represent the experimental data of Leonard et al. (11). The solid line represents the cross section calculated with the resonance parameters.

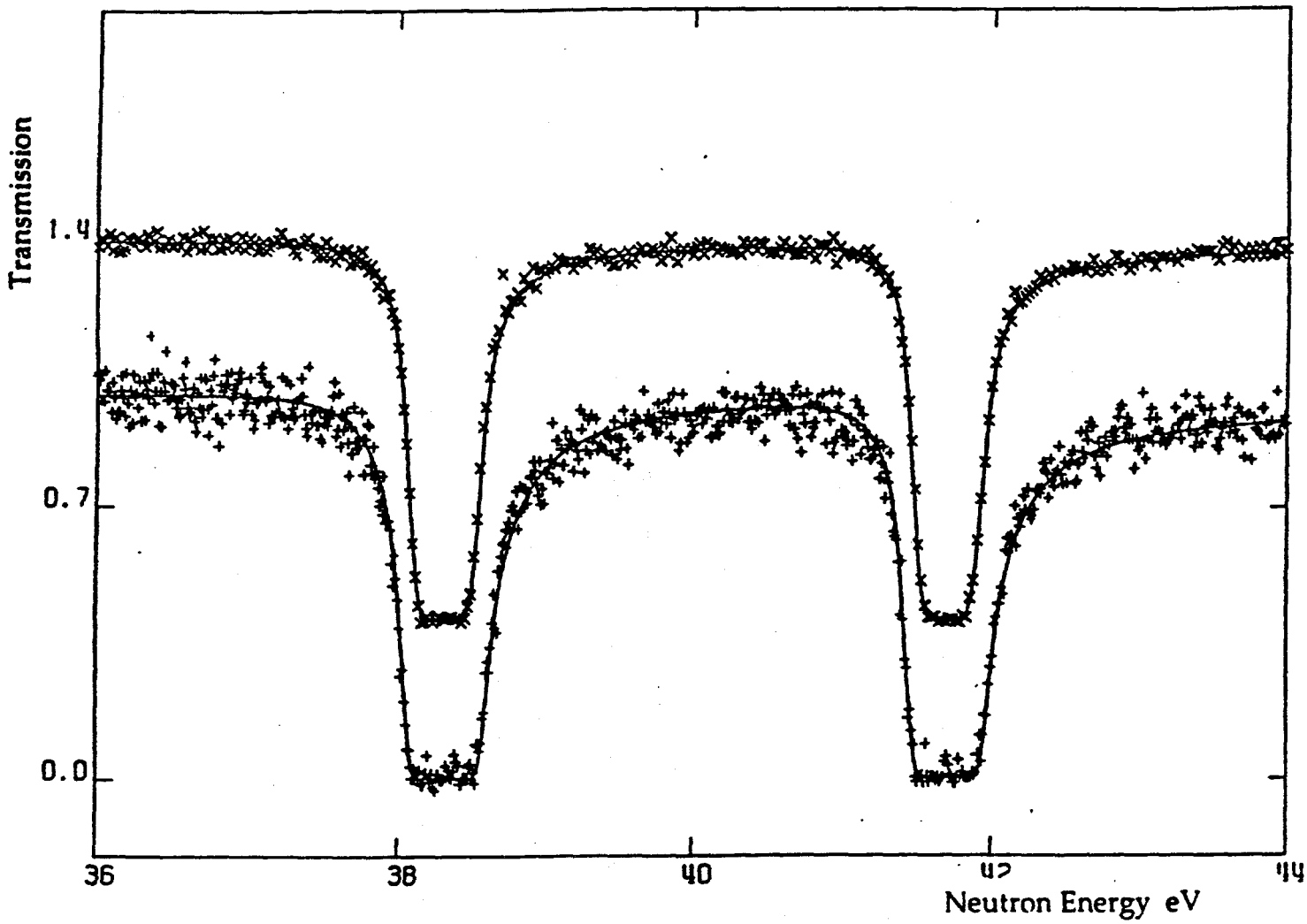

Figure 4- Transmission data in the energy interval from 36 eV to 44 eV.The crosses represent the experimental data of Kolar et al. (2). The solid line represents the values calculated with the resonance parameters.The transmission data of the thin sample were displaced by 0.5 for clarity of display.

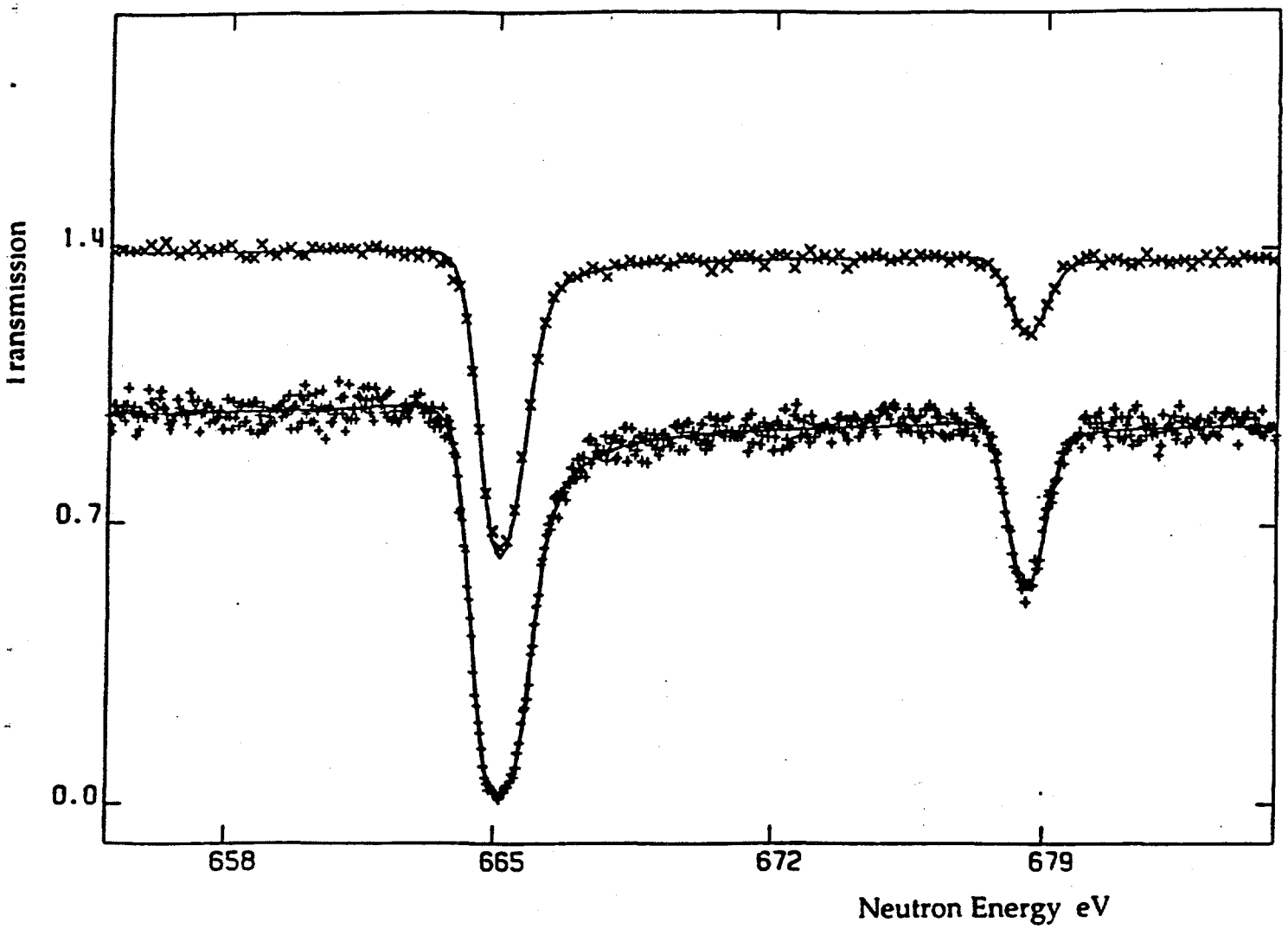

Figure 5- Transmission data in the energy interval from 653 eV to 685 eV.The crosses represent the experimental data of Kolar et al. (2). The solid line represents the data calculated with the resonance parameters. The transmission data of the thin sample were displaced by 0.5 for clarity of the display.

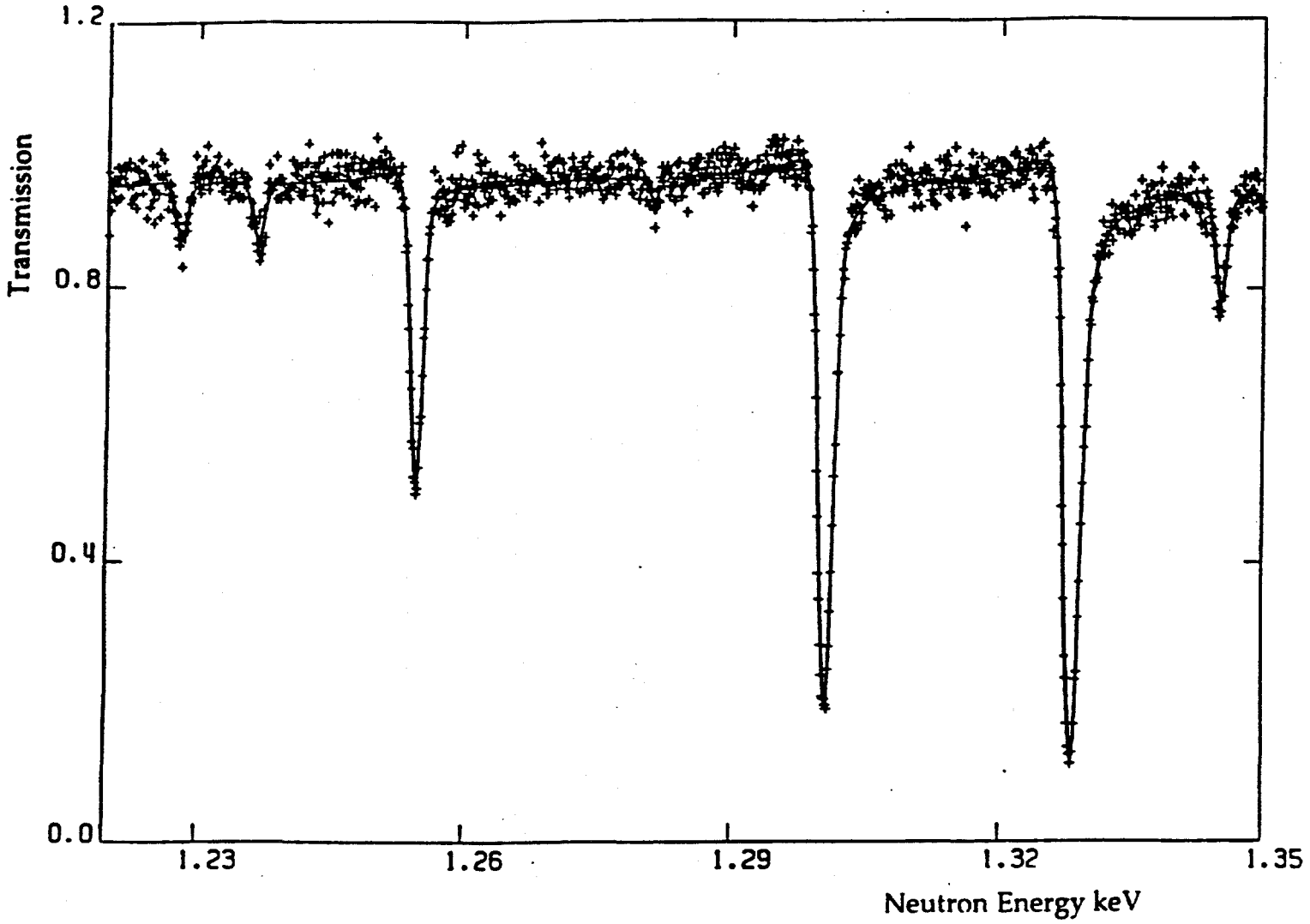

Figure 6- Transmission data in the energy interval from 1.20 keV to 1.35 keV. The crosses represent the experimental data of Kolar et al. (2). The solid line represents the data calculated with the resonance parameters.

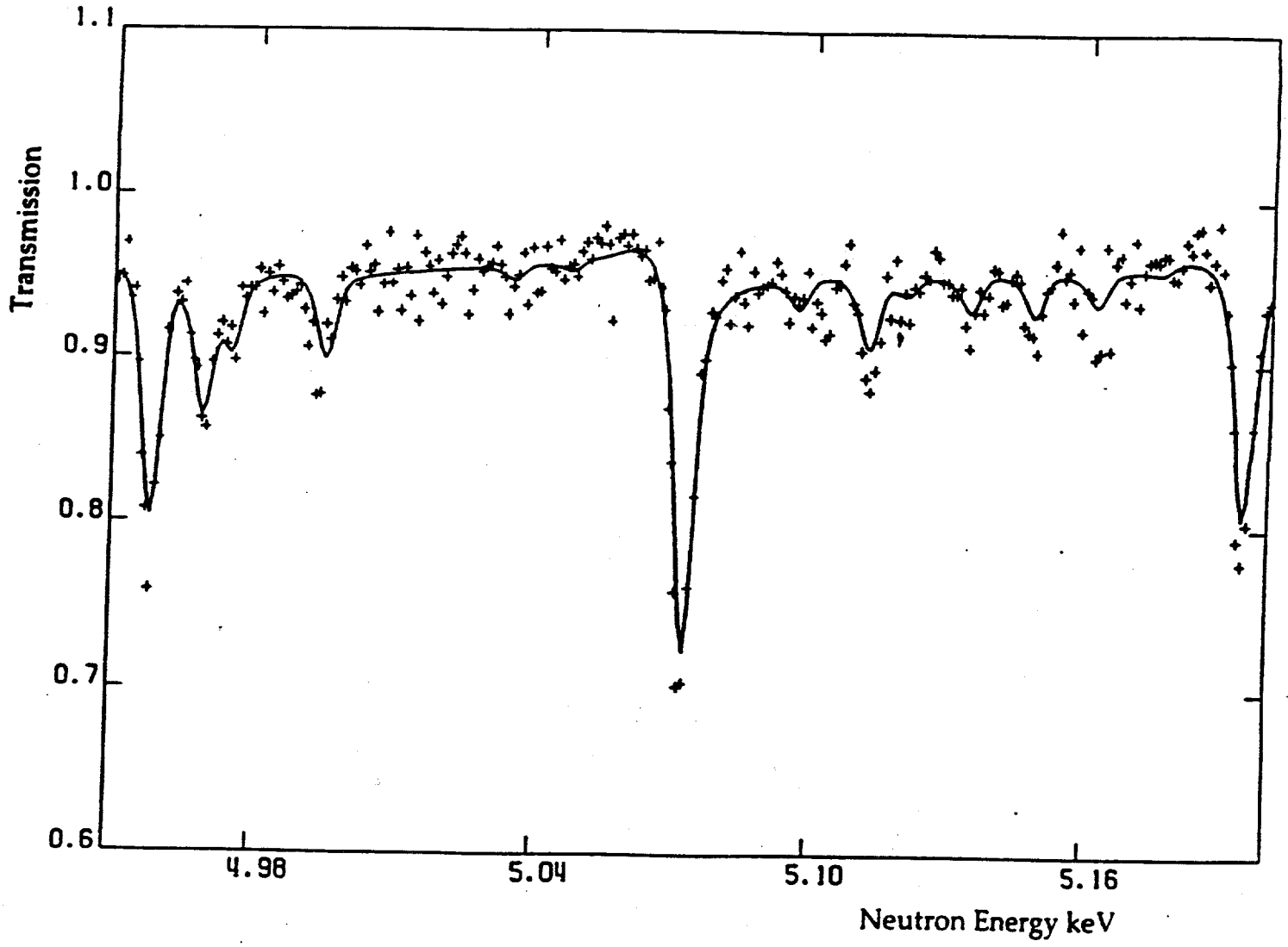

Figure 7- Transmission data in the energy interval from 4.95 keV to 5.20 keV. The crosses are the experimental data of Kolar et al. (2). The solid line represents the data calculated with the resonance parameters.

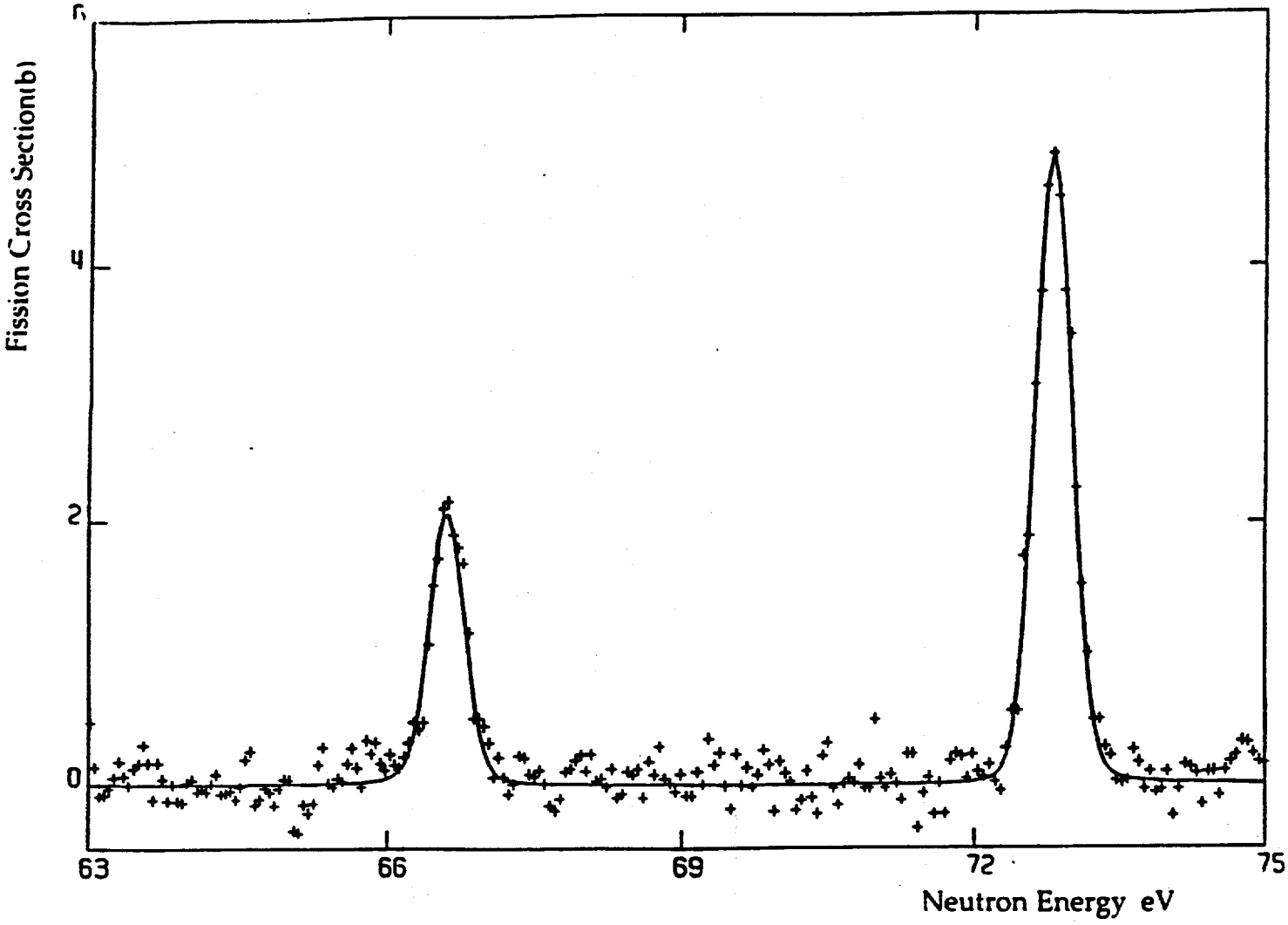

Figure 8- The fission cross-section in the energy interval from 63 eV to 65 eV. The crosses represent the experimental data of Weston et al. (3). The solid line represents the data calculated with the resonance parameters.

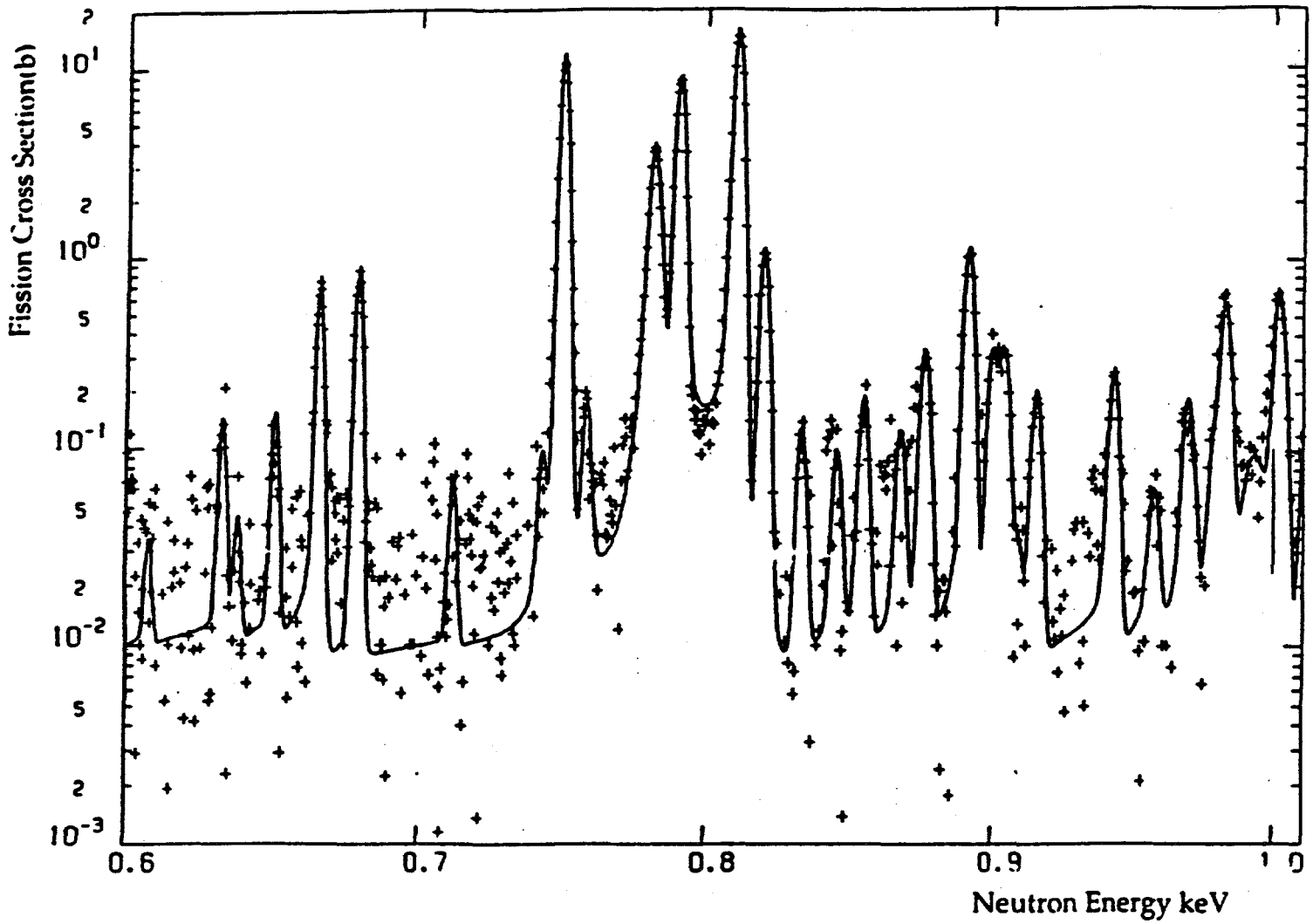

Figure 9- The fission cross section in the energy interval from 0.6 keV to 1.0 keV. The crosses represent the experimental data of Weston et al. (3). The solid line represents the cross section calculated with the resonance parameters.

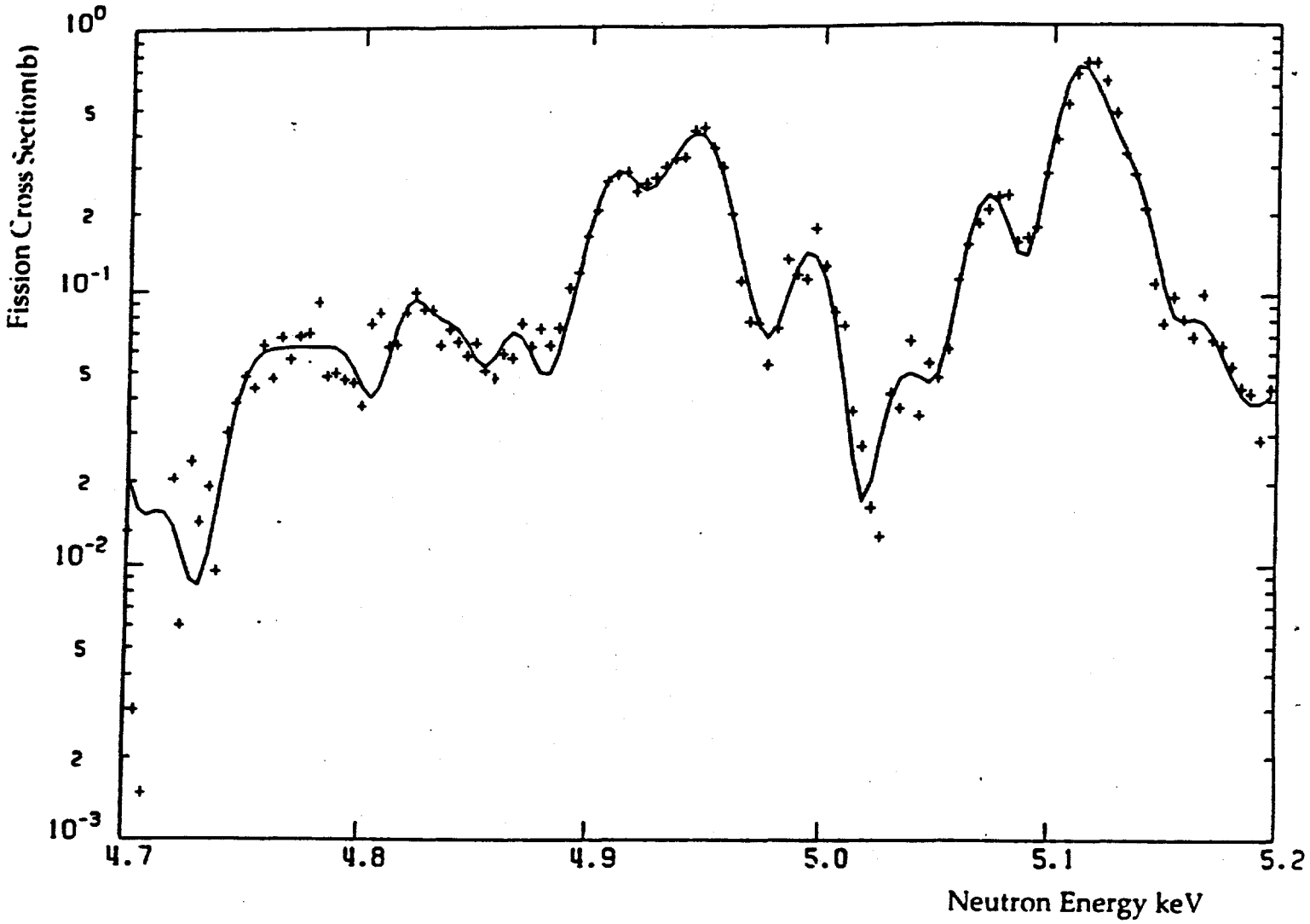

Figure 10- The fission cross section in the energy interval from 4.7 keV to 5.2 keV.The crosses represent the experimental data of Weston et al.(3).The solid line represents the cross section calculated with the resonance parameters.

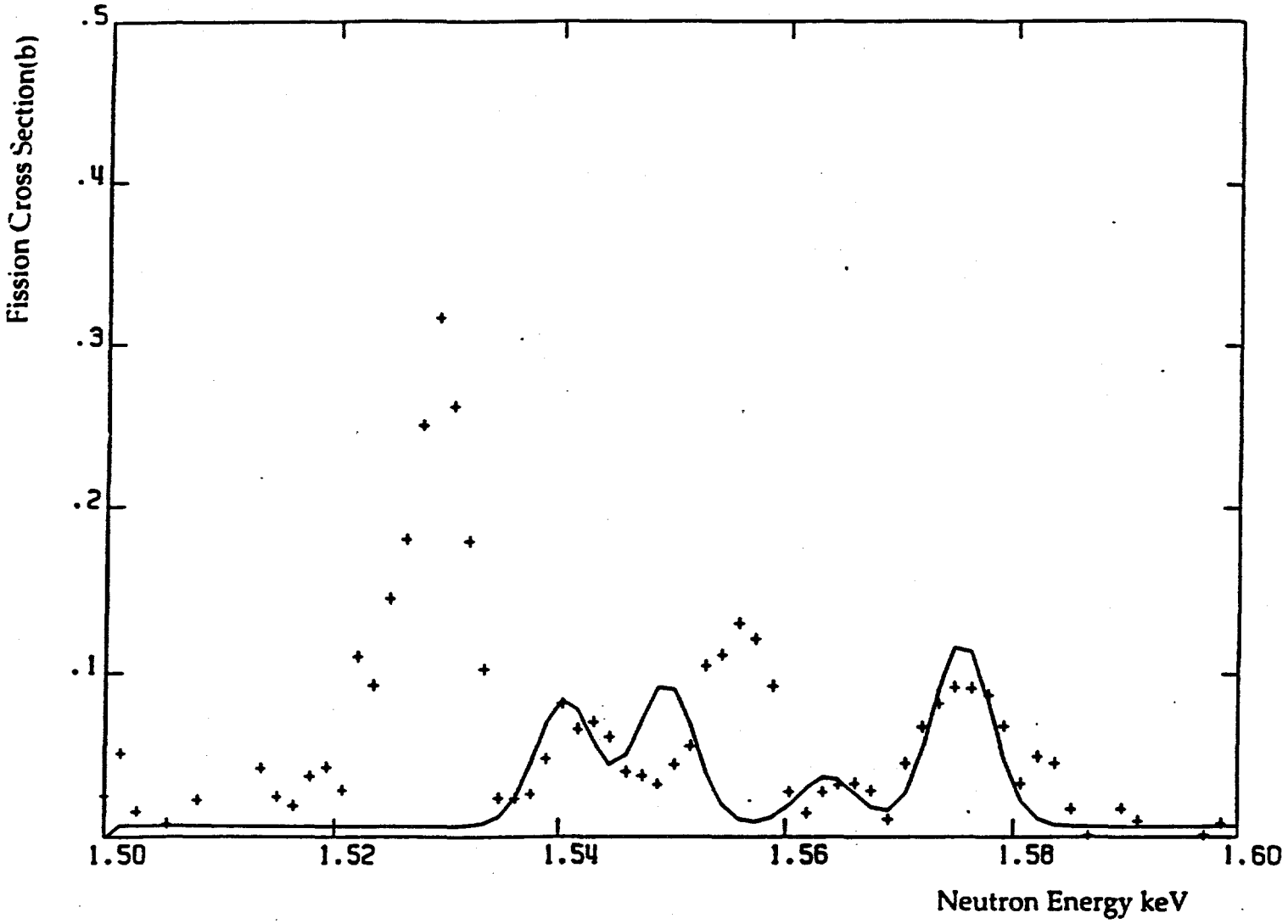

Figure 11- The fission cross-section in the energy interval from 1.50 keV to 1.60 keV. The crosses represent the experimental data of Weston et al. (3). The solid line represents the data calculated with the resonance parameters of ENDF/B-VI. The 4 resonances of the theoretical curve correspond to those identified by Kolar et al. (2) from transmission measurements.

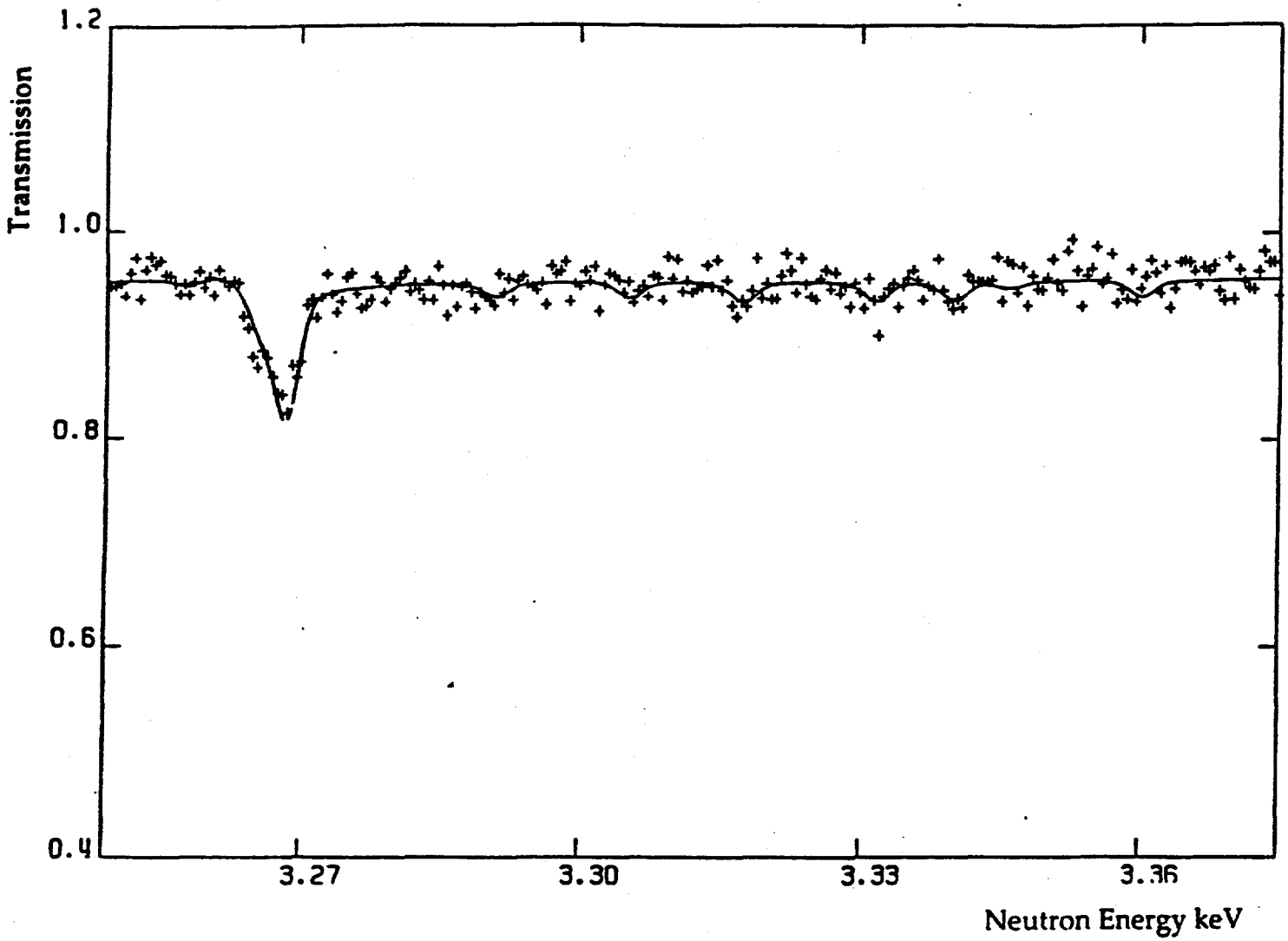

- Figure 12- Transmission data in the energy interval from 3.250 keV to 3.375 keV. The crosses represent the experimental data of Kolar et al. (2).The solid line represents the data calculated with the resonance parameters.Only the resonances at 3268.5 eV and 3332.0 eV were identified by Kolar et al. (2) and used for ENDF/B-VI.In the present work, 8 additional resonances are proposed, giving a realistic average spacing of 12 eV in the corresponding energy interval.

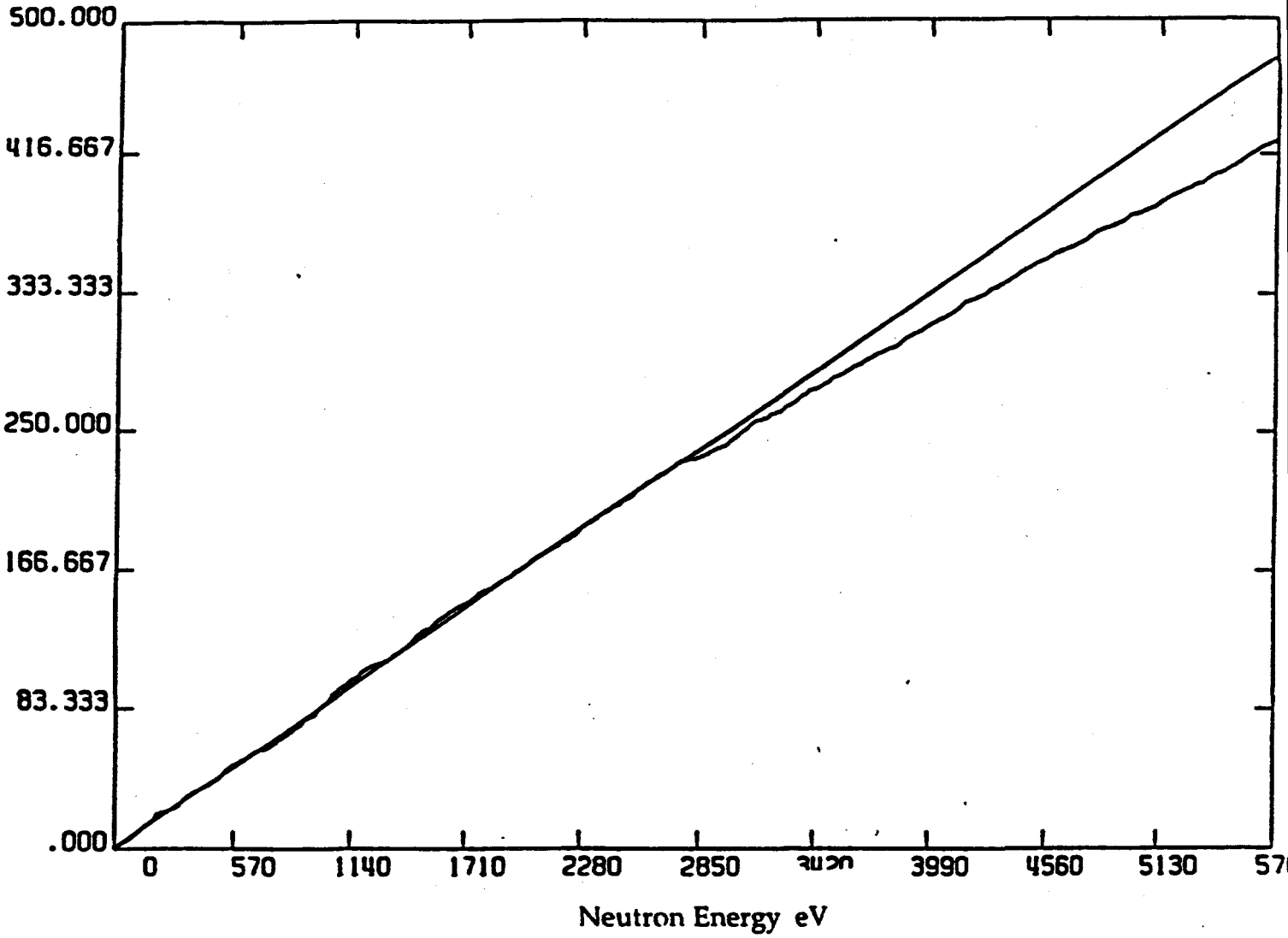

Figure 13- The number N of resonances identified in the energy range from 0 eV to E eV as a function of E.On the average,the variation of N is linear in the energy range from 0 eV to about 2750 eV with an average spacing of 12.06 eV.Beyond this energy, a large number of small resonances is still missing.

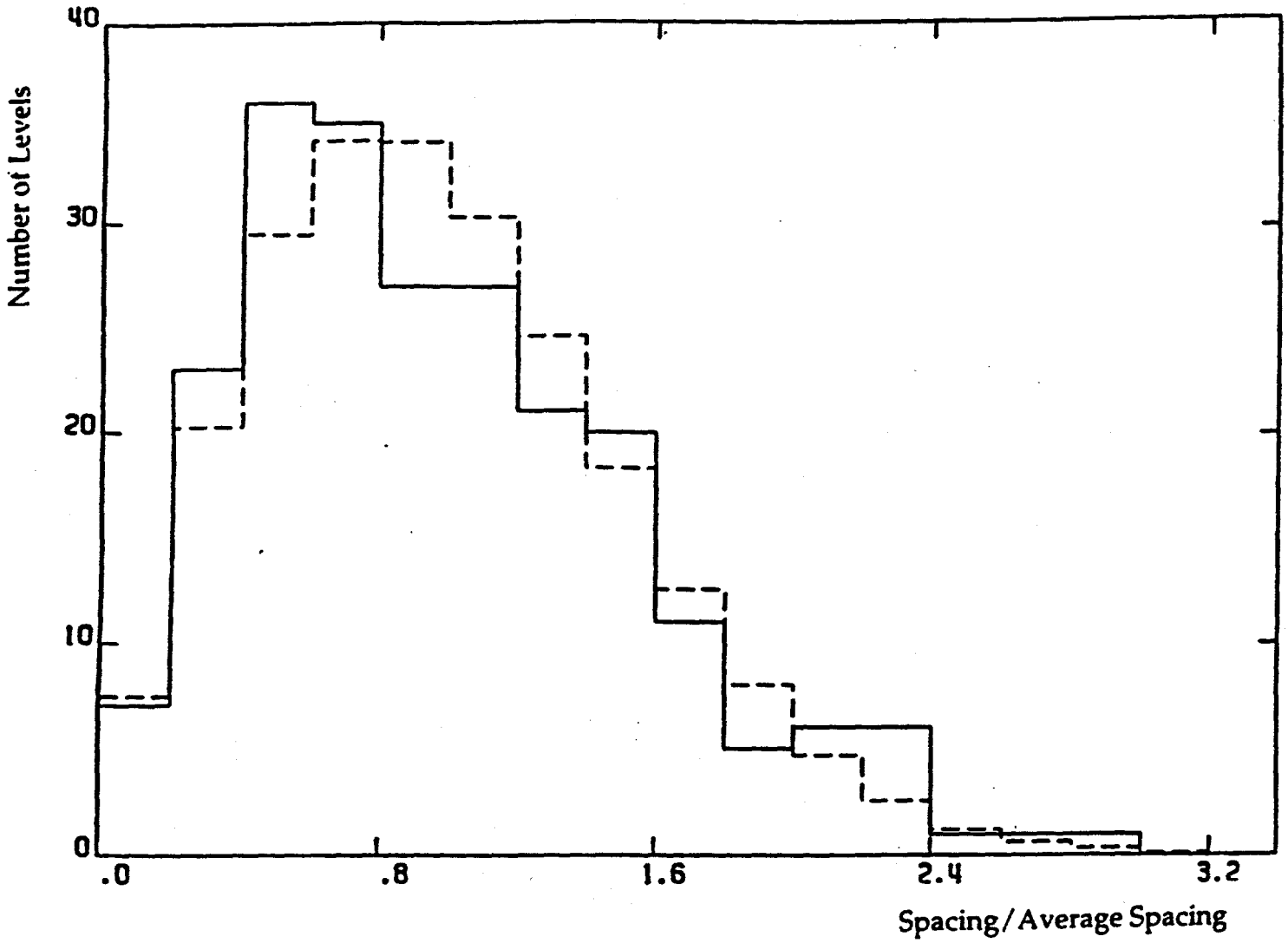

Figure 14- Differential distribution of the spacings of the resonances. The solid line represents the histogram of the experimental data.The dotted line is the Wigner theoretical distribution.

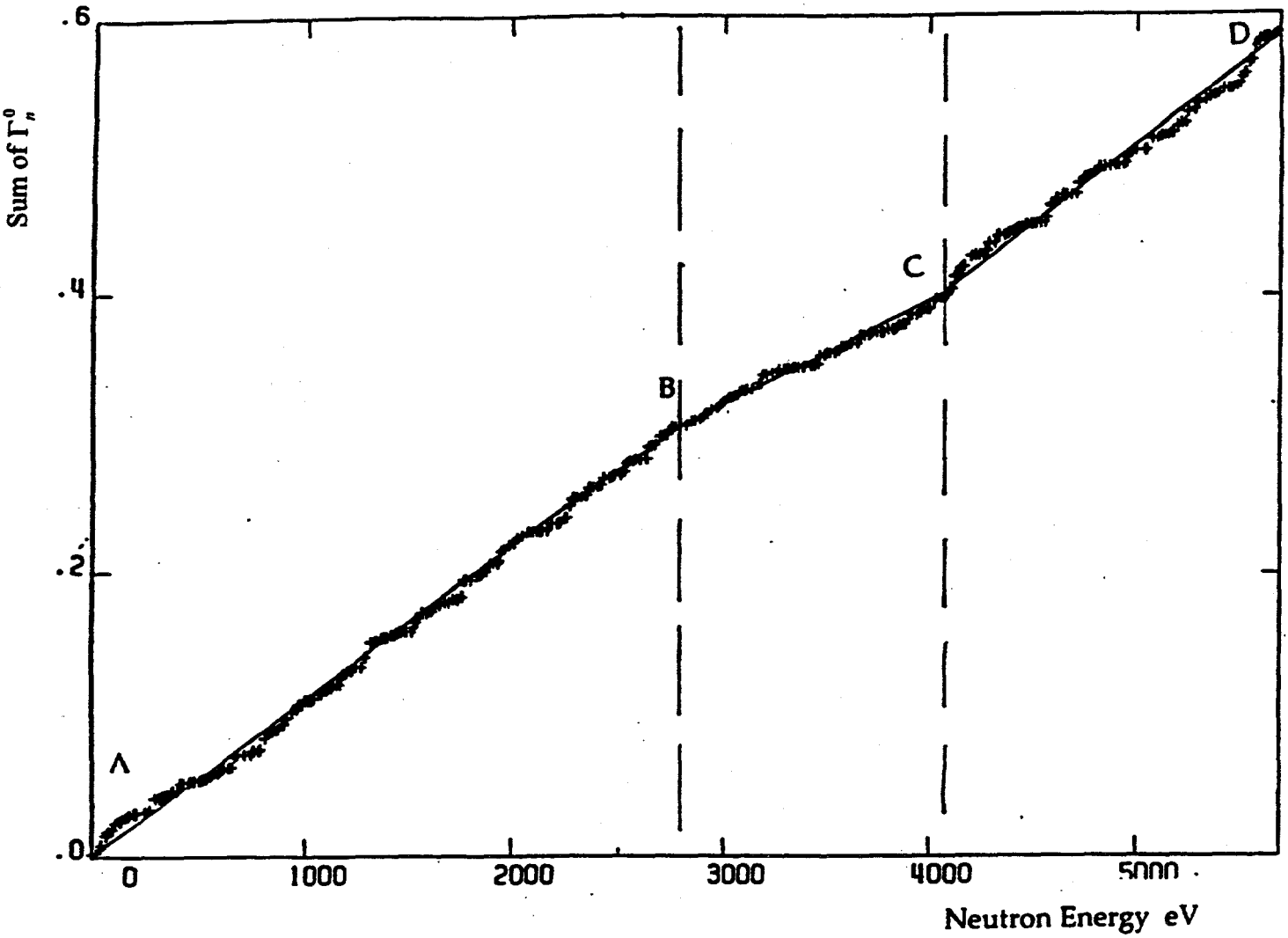

Figure 15- Variation of the sum of the reduced neutron widths as a function of energy.The experimental histogram shows three parts with different slopes.The parts AB, BC, and CD correspond to the strength functions 1.069×10^{-4}, 0.696×10^{-4} and 1.158×10^{-4} respectively.

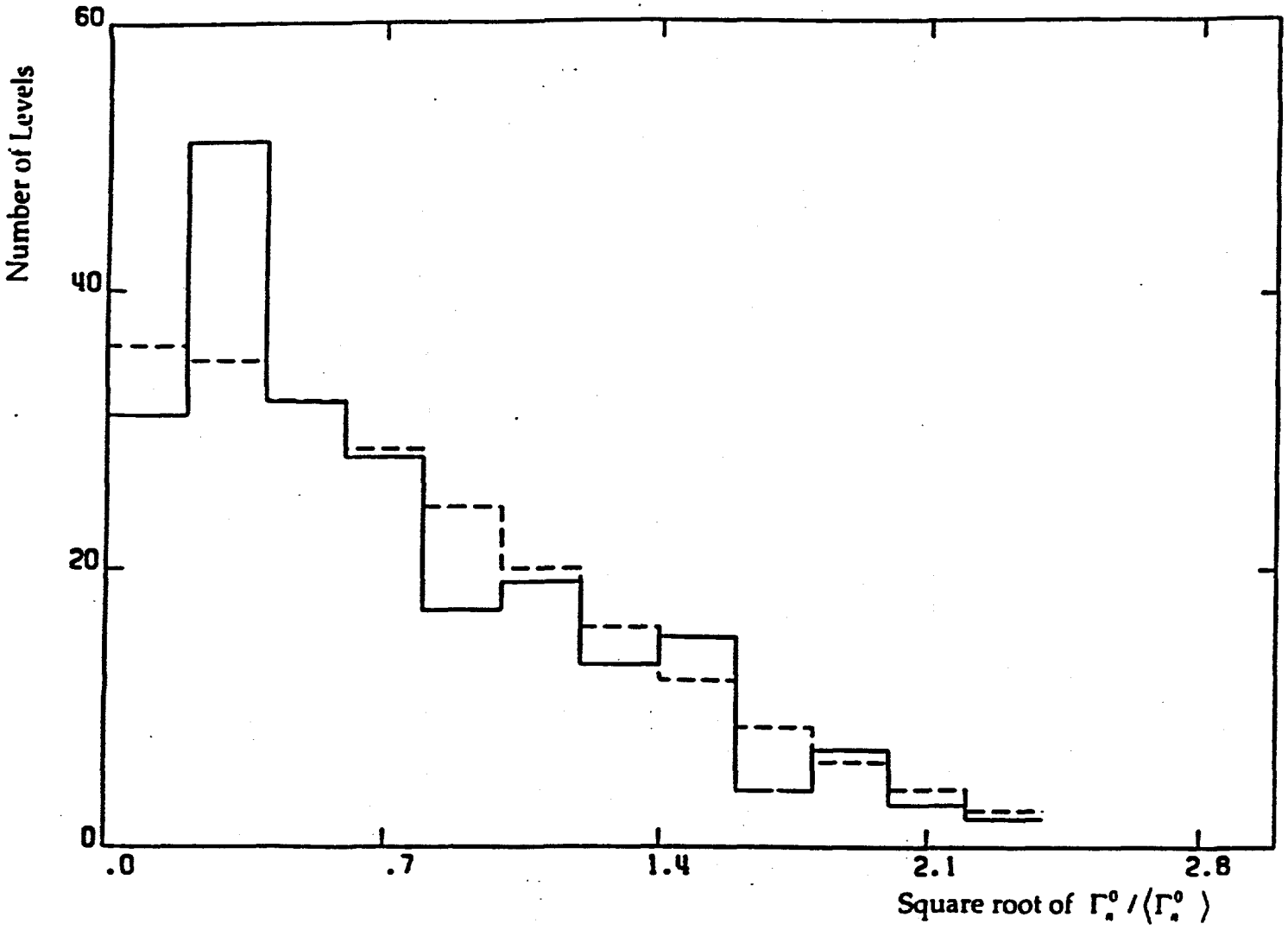

Figure 16- Differential distribution of the reduced neutron widths of the resonances at energies below 2750 eV. The solid line corresponds to the experimental histogram and the dotted line shows the corresponding PorterThomas distribution.

APPENDIX

240-Pu Resonance Parameters			
Energy (eV)	Width		
	Capture (meV)	Neutron (meV)	Fission (meV)
0.4071E+04	0.3180E+02	0.3551E+05	0.3372E-02
0.1305E+04	0.3180E+02	0.3522E+04	-0.4305E-01
0.3051E+03	0.3180E+02	0.2142E+03	0.4000E-01
0.7006E+02	0.3180E+02	0.3091E+03	-0.4000E-01
0.5794E+04	0.3180E+02	0.3342E+04	0.4000E-01
0.6002E+04	0.3180E+02	0.1272E+04	0.4000E-01
0.6986E+04	0.3180E+02	0.1100E+05	0.4000E-01
0.9901E+04	0.3180E+02	0.4825E+05	0.4000E-01
0.1445E+02	0.3100E+02	0.4586E+01	0.9000E-02
0.1056E+01	0.3060E+02	0.2450E+01	0.8501E-02
0.2043E+02	0.2698E+02	0.2750E+01	-0.2034E+00
0.3831E+02	0.2400E+02	0.1959E+02	0.9500E-02
0.4169E+02	0.2548E+02	0.1745E+02	-0.3372E-02
0.6662E+02	0.3302E+02	0.5549E+02	0.2585E-01
0.7279E+02	0.2639E+02	0.2173E+02	0.9000E-01
0.9078E+02	0.3079E+02	0.1327E+02	-0.1012E-01
0.9249E+02	0.2826E+02	0.3004E+01	-0.6317E-01
0.1050E+03	0.2855E+02	0.4621E+02	-0.5097E-02
0.1216E+03	0.3356E+02	0.1493E+02	0.4300E-01
0.1257E+03	0.3180E+02	0.1200E+00	-0.2000E-01
0.1308E+03	0.3086E+02	0.1787E+00	0.2413E+00
0.1353E+03	0.3289E+02	0.1828E+02	0.2636E-01
0.1520E+03	0.3746E+02	0.1349E+02	0.3568E+00

240-Pu Resonance Parameters (Contd.)

Energy (eV)	Width		
	Capture (meV)	Neutron (meV)	Fission (meV)
0.1627E+03	0.2911E+02	0.8484E+01	-0.5208E-02
0.1701E+03	0.3104E+02	0.1325E+02	-0.1349E+00
0.1858E+03	0.3096E+02	0.1578E+02	0.8954E-02
.1920E+03	0.3065E+02	0.2851E+00	-0.1284E+00
.1956E+03	0.3180E+02	0.1600E+00	0.1200E+00
.1974E+03	0.3180E+02	0.1600E+00	-0.1200E+00
.1997E+03	0.2860E+02	0.9700E+00	0.1373E+00
.2391E+03	0.2873E+02	0.1191E+02	0.4086E-01
.2603E+03	0.3278E+02	0.2225E+02	-0.9113E-01
.2870E+03	0.3204E+02	0.1346E+03	-0.3772E+00
.3048E+03	0.3387E+02	0.7367E+01	0.6924E-01
.3136E+03	0.3180E+02	0.1200E+00	-0.3000E+00
.3182E+03	0.3219E+02	0.5230E+01	0.1400E+00
.3206E+03	0.3488E+02	0.1891E+02	-0.5570E-01
.3327E+03	0.3180E+02	0.1300E+00	0.2000E-01
0.3383E+03	0.3139E+02	0.5938E+01	-0.5842E-02
0.3459E+03	0.3392E+02	0.1590E+02	0.1386E+00
0.3637E+03	0.3883E+02	0.3163E+02	0.2447E-01
0.3719E+03	0.3037E+02	0.1329E+02	-0.4024E-01
0.3930E+03	0.3180E+02	0.1500E+00	-0.2000E-01
0.4049E+03	0.3241E+02	0.1033E+03	-0.4717E+00
0.4189E+03	0.3091E+02	0.5769E+01	0.7077E-01
0.4457E+03	0.3137E+02	0.1845E+01	-0.2210E+00
0.4497E+03	0.3218E+02	0.1610E+02	0.4316E-01
0.4665E+03	0.3290E+02	0.2651E+01	0.3438E+00

240-Pu Resonance Parameters (Contd.)

Energy (eV)	Width		
	Capture (meV)	Neutron (meV)	Fission (meV)
0.4733E+03	0.3070E+02	0.4113E+01	0.0000E+00
0.4938E+03	0.3153E+02	0.5346E+01	-0.1218E+00
0.4992E+03	0.3632E+02	0.1855E+02	0.1219E+00
0.5100E+03	0.3180E+02	0.4140E+00	0.5000E-01
0.5125E+03	0.3180E+02	0.5175E+00	-0.5000E-01
0.5142E+03	0.3360E+02	0.2085E+02	-0.7429E-01
0.5263E+03	0.3180E+02	0.9607E+00	0.0000E+00
0.5308E+03	0.3180E+02	0.6768E+00	0.4800E+00
0.5464E+03	0.3990E+02	0.3106E+02	-0.3873E-01
0.5531E+03	0.3478E+02	0.1787E+02	0.2168E+00
0.5662E+03	0.3381E+02	0.3135E+02	-0.1830E+00
0.5842E+03	0.3180E+02	0.1152E+01	0.7700E+00
0.5967E+03	0.3717E+02	0.5421E+02	0.4478E-01
0.6080E+03	0.2915E+02	0.2222E+02	-0.2107E-01
0.6325E+03	0.3243E+02	0.1350E+02	-0.1836E+00
0.6376E+03	0.3060E+02	0.1188E+02	-0.5091E-01
0.6499E+03	0.3180E+02	0.1200E+01	0.1700E+01
0.6651E+03	0.2738E+02	0.2033E+03	-0.3856E+00
0.6785E+03	0.3203E+02	0.2540E+02	-0.8989E+00
0.7121E+03	0.3180E+02	0.1330E+01	0.7806E+00
0.7433E+03	0.3180E+02	0.1010E+01	0.1370E+01
0.7501E+03	0.3248E+02	0.6952E+02	-0.1132E+02
0.7589E+03	0.3203E+02	0.5822E+01	0.5764E+00
0.7783E+03	0.3180E+02	0.1120E+01	0.5700E+00
0.7824E+03	0.3123E+02	0.3832E+01	-0.1859E+04

240-Pu Resonance Parameters (Contd.)

Energy (eV)	Width		
	Capture (meV)	Neutron (meV)	Fission (meV)
0.7908E+03	0.2317E+02	0.2524E+02	-0.1399E+02
0.8105E+03	0.3728E+02	0.2197E+03	0.1398E+02
0.8199E+03	0.2981E+02	0.1106E+03	0.1008E+01
0.8333E+03	0.3180E+02	0.1020E+01	-0.3000E+01
0.8456E+03	0.3356E+02	0.9483E+01	0.2999E+00
0.8548E+03	0.3467E+02	0.4710E+02	-0.2401E+00
0.8680E+03	0.3180E+02	0.1020E+01	0.3000E+01
0.8764E+03	0.3286E+02	0.1452E+02	0.8688E+00
0.8915E+03	0.3226E+02	0.9468E+02	-0.1275E+01
0.9000E+03	0.3180E+02	0.1000E+01	-0.1200E+02
0.9040E+03	0.3477E+02	0.2208E+02	-0.7322E+00
0.9089E+03	0.3220E+02	0.7787E+02	0.3237E-01
0.9152E+03	0.3483E+02	0.3588E+02	-0.3398E+00
0.9435E+03	0.3274E+02	0.1228E+03	-0.2977E+00
0.9584E+03	0.3098E+02	0.7392E+02	0.7036E-01
0.9700E+03	0.3180E+02	0.1000E+01	0.5000E+01
0.9713E+03	0.2989E+02	0.7979E+02	0.6005E-01
0.9792E+03	0.3180E+02	0.7200E+01	-0.4366E+00
0.9830E+03	0.3180E+02	0.1000E+01	0.4800E+02
0.9930E+03	0.3180E+02	0.3000E+00	0.8000E+04
0.1002E+04	0.2979E+02	0.9726E+02	-0.1079E+01
0.1012E+04	0.3180E+02	0.2000E+01	0.7322E+01
0.1024E+04	0.3180E+02	0.5231E+01	0.4555E+00
0.1029E+04	0.3180E+02	0.2000E+01	0.6534E+01
0.1037E+04	0.3180E+02	0.2000E+01	-0.3366E+01

240-Pu Resonance Parameters (Contd.)

Energy (eV)	Width		
	Capture (meV)	Neutron (meV)	Fission (meV)
0.1042E+04	0.2974E+02	0.1214E+02	-0.1599E+00
0.1046E+04	0.3180E+02	0.3939E+01	0.1085E+01
0.1051E+04	0.3180E+02	0.2000E+01	0.1284E+02
0.1073E+04	0.2909E+02	0.1092E+03	-0.1840E+00
0.1077E+04	0.3180E+02	0.1700E+01	-0.3425E+01
0.1086E+04	0.3180E+02	0.2000E+01	0.2122E+01
0.1100E+04	0.3408E+02	0.8003E+02	-0.2770E+00
0.1116E+04	0.3180E+02	0.2571E+01	-0.3400E+00
0.1129E+04	0.3095E+02	0.4979E+02	0.6977E+00
0.1134E+04	0.3180E+02	0.6965E+01	0.2397E+00
0.1143E+04	0.3098E+02	0.4220E+02	-0.1214E+00
0.1160E+04	0.3286E+02	0.2379E+02	-0.3076E+00
0.1176E+04	0.3180E+02	0.1500E+01	0.2770E+01
0.1186E+04	0.3212E+02	0.1588E+03	0.1237E+00
0.1191E+04	0.3183E+02	0.1141E+03	-0.1786E+00
0.1201E+04	0.3180E+02	0.2000E+01	0.2120E+01
0.1209E+04	0.3170E+02	0.6254E+02	-0.1160E+00
0.1228E+04	0.3180E+02	0.1039E+02	0.4000E+00
0.1237E+04	0.3180E+02	0.1118E+02	0.4150E+00
0.1255E+04	0.3119E+02	0.7985E+02	-0.1624E+01
0.1281E+04	0.3180E+02	0.4201E+01	-0.4100E+00
0.1300E+04	0.3065E+02	0.2491E+03	-0.9150E+00
0.1328E+04	0.3271E+02	0.3675E+03	0.6805E+00
0.1345E+04	0.3180E+02	0.2491E+02	0.4534E+00
0.1351E+04	0.3180E+02	0.7739E+01	-0.3000E-01

240-Pu Resonance Parameters (Contd.)

Energy (eV)	Width		
	Capture (meV)	Neutron (meV)	Fission (meV)
0.1363E+04	0.3180E+02	0.7312E+01	0.1262E+01
0.1377E+04	0.3123E+02	0.6614E+02	-0.9683E+00
0.1389E+04	0.3180E+02	0.1467E+02	0.6296E+01
0.1402E+04	0.3180E+02	0.9830E+01	-0.2086E+04
0.1408E+04	0.3180E+02	0.9910E+01	-0.8520E+02
0.1426E+04	0.2987E+02	0.3908E+02	0.5485E+01
0.1429E+04	0.3180E+02	0.1569E+02	-0.2226E+01
0.1442E+04	0.3180E+02	0.2000E+01	0.9000E+01
0.1450E+04	0.3180E+02	0.2691E+02	-0.2028E+01
0.1451E+04	0.3152E+02	0.2741E+02	-0.2181E+01
0.1463E+04	0.3180E+02	0.2180E+02	0.1070E+01
0.1466E+04	0.3180E+02	0.2000E+01	-0.1170E+02
0.1475E+04	0.3180E+02	0.2000E+01	-0.9000E+01
0.1481E+04	0.3180E+02	0.9762E+01	0.1241E+01
0.1498E+04	0.3180E+02	0.2000E+01	0.2500E+01
0.1503E+04	0.3180E+02	0.4000E+01	-0.1000E+00
0.1529E+04	0.3180E+02	0.5000E+01	0.6477E+01
0.1541E+04	0.3231E+02	0.1025E+03	-0.2800E+00
0.1549E+04	0.3171E+02	0.1617E+03	0.1509E+00
0.1555E+04	0.3180E+02	0.2500E+01	-0.4649E+01
0.1564E+04	0.3044E+02	0.1180E+03	-0.1000E+00
0.1575E+04	0.3164E+02	0.1265E+03	-0.3460E+00
0.1582E+04	0.3180E+02	0.3000E+01	0.1000E+00
0.1600E+04	0.3180E+02	0.2000E+01	-0.1000E+00
0.1610E+04	0.3180E+02	0.3599E+02	0.6809E+00

240-Pu Resonance Parameters (Contd.)

Energy (eV)	Width		
	Capture (meV)	Neutron (meV)	Fission (meV)
0.1622E+04	0.3180E+02	0.2796E+02	-0.2900E+00
0.1629E+04	0.3180E+02	0.5000E+01	0.9018E+00
0.1643E+04	0.3166E+02	0.1110E+03	0.1610E+00
0.1663E+04	0.3218E+02	0.6912E+02	-0.3779E+00
0.1667E+04	0.3180E+02	0.6000E+01	0.1000E+00
0.1688E+04	0.3180E+02	0.3526E+02	-0.6553E+00
0.1707E+04	0.3180E+02	0.4500E+01	0.1000E+01
0.1724E+04	0.3144E+02	0.8441E+02	0.2140E+01
0.1749E+04	0.3180E+02	0.3000E+01	-0.1000E+00
0.1742E+04	0.3180E+02	0.2484E+02	0.6095E+00
0.1764E+04	0.3180E+02	0.5549E+02	-0.5780E+00
0.1771E+04	0.3180E+02	0.9730E+01	0.1100E+00
0.1779E+04	0.3065E+02	0.4871E+03	-0.8529E-01
0.1789E+04	0.3180E+02	0.5000E+01	0.1657E+01
0.1811E+04	0.3180E+02	0.5000E+01	0.1755E+01
0.1842E+04	0.3306E+02	0.1282E+03	-0.1035E+02
0.1853E+04	0.3180E+02	0.3392E+02	-0.3640E+01
0.1862E+04	0.3180E+02	0.4000E+01	-0.1005E+00
0.1873E+04	0.3074E+02	0.8065E+02	0.4163E+01
0.1886E+04	0.3180E+02	0.5000E+01	-0.1396E+01
0.1902E+04	0.3063E+02	0.2180E+03	0.3296E+01
0.1917E+04	0.3180E+02	0.3519E+02	0.9562E+02
0.1937E+04	0.3180E+02	0.1980E+01	-0.1810E+04
0.1943E+04	0.3180E+02	0.7931E+01	0.6096E+01
0.1949E+04	0.3180E+02	0.8586E+02	0.8835E+01

240-Pu Resonance Parameters (Contd.)

Energy (eV)	Width		
	Capture (meV)	Neutron (meV)	Fission (meV)
0.1956E+04	0.3084E+02	0.2762E+03	-0.2437E+02
0.1973E+04	0.3180E+02	0.7159E+02	0.1898E+01
0.1991E+04	0.3067E+02	0.1176E+03	-0.5576E-01
0.1999E+04	0.3180E+02	0.5398E+01	0.4983E-01
0.2017E+04	0.3151E+02	0.5500E+02	-0.1501E+01
0.2023E+04	0.2871E+02	0.6019E+02	0.1340E+01
0.2033E+04	0.3230E+02	0.1112E+03	0.9078E+01
0.2038E+04	0.3180E+02	0.5000E+01	0.1000E+00
0.2056E+04	0.2844E+02	0.7248E+02	-0.5398E+01
0.2061E+04	0.3100E+02	0.5000E+01	0.1000E+00
0.2083E+04	0.3088E+02	0.9914E+02	-0.9000E-01
0.2097E+04	0.3180E+02	0.1000E+02	0.9000E+00
0.2111E+04	0.3180E+02	0.1388E+02	-0.1040E+01
0.2127E+04	0.3180E+02	0.6000E+01	-0.7000E+00
0.2142E+04	0.3180E+02	0.8000E+01	-0.9000E+00
0.2155E+04	0.3180E+02	0.1405E+02	0.1164E+01
0.2177E+04	0.3180E+02	0.1000E+02	0.1000E+01
0.2182E+04	0.3006E+02	0.8963E+02	0.9940E-01
0.2198E+04	0.3067E+02	0.1398E+03	-0.1400E+00
0.2223E+04	0.3180E+02	0.1200E+02	-0.1000E+00
0.2230E+04	0.3180E+02	0.9000E+01	0.1000E+00
0.2241E+04	0.3180E+02	0.3412E+02	-0.2200E+00
0.2257E+04	0.3099E+02	0.1367E+03	0.1900E+00
0.2263E+04	0.3180E+02	0.1000E+02	-0.1000E+00
0.2268E+04	0.3180E+02	0.8000E+01	0.1000E+00

240-Pu Resonance Parameters (Contd.)

Energy (eV)	Width		
	Capture (meV)	Neutron (meV)	Fission (meV)
0.2278E+04	0.3160E+02	0.3983E+03	0.2400E+00
0.2283E+04	0.3100E+02	0.2793E+02	0.4000E+00
0.2291E+04	0.3088E+02	0.2183E+03	-0.1100E+00
0.2303E+04	0.3180E+02	0.1695E+02	-0.8000E-01
0.2318E+04	0.3180E+02	0.1000E+02	-0.1400E+01
0.2334E+04	0.3180E+02	0.3784E+02	0.2600E+00
0.2351E+04	0.3180E+02	0.3854E+02	0.1000E+00
0.2360E+04	0.3180E+02	0.1200E+02	-0.1000E+00
0.2366E+04	0.3048E+02	0.2429E+03	0.1500E+00
0.2373E+04	0.3180E+02	0.9655E+01	-0.9000E-01
0.2386E+04	0.3180E+02	0.1835E+02	0.5500E+00
0.2405E+04	0.3180E+02	0.2502E+02	-0.5000E-01
0.2416E+04	0.3180E+02	0.6835E+02	0.1900E+00
0.2425E+04	0.3180E+02	0.5000E+01	0.1000E+00
0.2434E+04	0.3044E+02	0.2154E+03	0.1500E+00
0.2459E+04	0.3180E+02	0.2634E+02	-0.2000E+00
0.2470E+04	0.3180E+02	0.4895E+02	-0.1200E+00
0.2477E+04	0.3180E+02	0.1000E+02	-0.1200E+01
0.2484E+04	0.3180E+02	0.2145E+02	0.2500E+00
0.2512E+04	0.3180E+02	0.1000E+02	-0.1000E+00
0.2521E+04	0.3380E+02	0.1142E+03	0.2800E+00
0.2531E+04	0.3180E+02	0.1500E+02	-0.1000E+00
0.2538E+04	0.3234E+02	0.2865E+03	0.3800E+00
0.2543E+04	0.3180E+02	0.7000E+00	0.1000E+00
0.2549E+04	0.3258E+02	0.8559E+02	-0.5200E+00

240-Pu Resonance Parameters (Contd.)

Energy (eV)	Width		
	Capture (meV)	Neutron (meV)	Fission (meV)
0.2563E+04	0.3180E+02	0.7000E+00	-0.1000E+00
0.2575E+04	0.3638E+02	0.4677E+02	-0.5924E+00
0.2578E+04	0.3180E+02	0.1000E+02	0.1000E+00
0.2596E+04	0.3180E+02	0.1000E+02	-0.1000E+01
0.2602E+04	0.3180E+02	0.1000E+02	0.5039E+01
0.2626E+04	0.3180E+02	0.1500E+02	-0.1000E+00
0.2633E+04	0.3180E+02	0.1000E+02	0.1000E+00
0.2639E+04	0.3162E+02	0.4298E+03	-0.4443E+01
0.2652E+04	0.3180E+02	0.3833E+02	0.1537E+02
0.2670E+04	0.3180E+02	0.1000E+02	-0.3933E+01
0.2693E+04	0.3180E+02	0.3261E+03	0.1107E+03
0.2696E+04	0.3180E+02	0.1500E+02	0.5807E+02
0.2707E+04	0.3180E+02	0.1000E+02	-0.1000E+02
0.2718E+04	0.3180E+02	0.4042E+02	0.2803E+01
0.2729E+04	0.3180E+02	0.1000E+02	-0.1000E+00
0.2739E+04	0.3180E+02	0.1817E+03	0.1020E+01
0.2749E+04	0.2913E+02	0.1135E+03	0.1143E+02
0.2764E+04	0.3180E+02	0.1000E+02	0.1000E+00
0.2817E+04	0.3180E+02	0.4435E+02	-0.1596E+01
0.2844E+04	0.3180E+02	0.1724E+03	-0.1277E+00
0.2858E+04	0.3180E+02	0.2866E+02	0.1522E+01
0.2882E+04	0.3180E+02	0.3198E+02	-0.3500E+00
0.2896E+04	0.3180E+02	0.6388E+02	0.1600E+00
0.2905E+04	0.3180E+02	0.1229E+03	0.6100E+00
0.2924E+04	0.3180E+02	0.1800E+02	-0.1000E+00

240-Pu Resonance Parameters (Contd.)

Energy (eV)	Width		
	Capture (meV)	Neutron (meV)	Fission (meV)
0.2938E+04	0.3180E+02	0.1532E+03	-0.4000E+00
0.2969E+04	0.3180E+02	0.9873E+02	-0.3600E+00
0.2980E+04	0.3180E+02	0.1125E+03	0.5000E-01
0.2987E+04	0.3180E+02	0.1089E+02	-0.9600E+00
0.2994E+04	0.3180E+02	0.6118E+02	0.2100E+00
0.3004E+04	0.3180E+02	0.8386E+02	0.3900E+00
0.3018E+04	0.3180E+02	0.1267E+03	-0.3200E+00
0.3030E+04	0.3180E+02	0.2013E+02	0.1310E+01
0.3040E+04	0.3180E+02	0.1000E+02	-0.3000E+00
0.3048E+04	0.3180E+02	0.1000E+02	0.3000E+00
0.3054E+04	0.3180E+02	0.4902E+02	-0.7980E+01
0.3069E+04	0.3180E+02	0.1367E+02	0.1323E+03
0.3078E+04	0.3180E+02	0.1334E+03	0.1068E+01
0.3088E+04	0.3180E+02	0.3346E+02	-0.1914E+01
0.3092E+04	0.3180E+02	0.1000E+02	-0.1002E+02
0.3106E+04	0.3180E+02	0.6000E+01	-0.1085E+02
0.3113E+04	0.3180E+02	0.3966E+02	0.7000E+00
0.3140E+04	0.3180E+02	0.4000E+01	-0.3500E+01
0.3173E+04	0.3180E+02	0.2393E+03	0.1190E+01
0.3185E+04	0.3180E+02	0.8000E+01	-0.3000E+00
0.3192E+04	0.3180E+02	0.3604E+03	0.4000E+00
0.3209E+04	0.3180E+02	0.1500E+02	0.3000E+00
0.3238E+04	0.3180E+02	0.7396E+02	-0.6400E+00
0.3258E+04	0.3180E+02	0.6000E+01	-0.3000E+00
0.3266E+04	0.3180E+02	0.2602E+02	0.1200E+00

240-Pu Resonance Parameters (Contd.)

Energy (eV)	Width		
	Capture (meV)	Neutron (meV)	Fission (meV)
0.3269E+04	0.3180E+02	0.1091E+03	0.1600E+00
0.3291E+04	0.3180E+02	0.1000E+02	-0.1500E+01
0.3306E+04	0.3180E+02	0.1200E+02	-0.1100E+01
0.3317E+04	0.3180E+02	0.1500E+02	0.3000E+00
0.3332E+04	0.3180E+02	0.1476E+02	-0.1428E+01
0.3340E+04	0.3180E+02	0.1400E+02	0.2497E+01
0.3346E+04	0.3180E+02	0.5000E+01	0.9805E+01
0.3360E+04	0.3180E+02	0.1300E+02	-0.8401E+01
0.3382E+04	0.3180E+02	0.1500E+02	-0.3000E+00
0.3382E+04	0.3180E+02	0.1595E+02	0.2265E+04
0.3389E+04	0.3180E+02	0.1500E+02	0.3000E+00
0.3423E+04	0.3180E+02	0.3514E+02	0.0000E+00
0.3440E+04	0.3180E+02	0.1000E+02	-0.3000E+00
0.3458E+04	0.3180E+02	0.7119E+02	-0.4342E+00
0.3466E+04	0.3180E+02	0.3646E+03	-0.8600E+00
0.3487E+04	0.3180E+02	0.2500E+02	0.3000E+00
0.3494E+04	0.3180E+02	0.6590E+02	-0.6600E+00
0.3500E+04	0.3180E+02	0.1000E+02	0.5000E+00
0.3514E+04	0.3180E+02	0.1000E+02	-0.5000E+00
0.3539E+04	0.3180E+02	0.1000E+02	0.5000E+00
0.3555E+04	0.3180E+02	0.9063E+02	0.0000E+00
0.3567E+04	0.3180E+02	0.1788E+03	-0.2561E+00
0.3581E+04	0.3180E+02	0.1500E+02	0.0000E+00
0.3595E+04	0.3180E+02	0.4218E+02	-0.3000E+00
0.3610E+04	0.3180E+02	0.7567E+02	0.3024E+00

240-Pu Resonance Parameters (Contd.)

Energy (eV)	Width		
	Capture (meV)	Neutron (meV)	Fission (meV)
0.3614E+04	0.3180E+02	0.3800E+02	0.3650E+00
0.3648E+04	0.3180E+02	0.1000E+02	0.2800E+00
0.3657E+04	0.3180E+02	0.2737E+03	-0.7984E-01
0.3665E+04	0.3180E+02	0.5414E+02	0.2833E+00
0.3682E+04	0.3180E+02	0.1000E+02	-0.9010E+00
0.3702E+04	0.3180E+02	0.5374E+02	0.9132E+00
0.3711E+04	0.3180E+02	0.2500E+02	-0.5000E+00
0.3723E+04	0.3180E+02	0.5576E+02	0.9400E+00
0.3743E+04	0.3180E+02	0.8000E+01	0.5000E+00
0.3765E+04	0.3180E+02	0.5000E+01	-0.5000E+00
0.3777E+04	0.3180E+02	0.5000E+01	-0.3245E+01
0.3800E+04	0.3180E+02	0.1079E+03	0.1144E+01
0.3823E+04	0.3180E+02	0.8000E+01	-0.4762E+00
0.3833E+04	0.3180E+02	0.4000E+01	-0.4839E+00
0.3844E+04	0.3180E+02	0.8033E+02	-0.9974E-01
0.3853E+04	0.3180E+02	0.1027E+03	0.3946E+00
0.3859E+04	0.3180E+02	0.1000E+02	0.2695E+01
0.3872E+04	0.3180E+02	0.4508E+02	0.1339E+01
0.3886E+04	0.3180E+02	0.1000E+02	-0.5000E+00
0.3901E+04	0.3180E+02	0.2296E+03	0.1100E+00
0.3916E+04	0.3180E+02	0.1825E+03	-0.2845E+00
0.3939E+04	0.3180E+02	0.1000E+02	0.9345E+00
0.3954E+04	0.3180E+02	0.1091E+03	-0.9120E+01
0.3960E+04	0.3180E+02	0.1000E+02	0.1000E+01
0.3975E+04	0.3180E+02	0.1189E+03	-0.1360E+01

240-Pu Resonance Parameters (Contd.)

Energy (eV)	Width		
	Capture (meV)	Neutron (meV)	Fission (meV)
0.3990E+04	0.3180E+02	0.2900E+02	0.9020E-01
0.4002E+04	0.3180E+02	0.2500E+02	-0.9962E+01
0.4022E+04	0.3180E+02	0.3547E+03	0.1112E+01
0.4031E+04	0.3180E+02	0.1130E+03	-0.3998E+00
0.4055E+04	0.3180E+02	0.2900E+02	0.3000E+00
0.4073E+04	0.3180E+02	0.7500E+01	0.3000E+00
0.4084E+04	0.3180E+02	0.1352E+03	-0.3100E+00
0.4100E+04	0.3180E+02	0.2900E+03	0.4687E+00
0.4110E+04	0.3180E+02	0.9000E+01	0.3000E+00
0.4122E+04	0.3180E+02	0.5421E+03	0.1573E+00
0.4135E+04	0.3180E+02	0.6788E+02	-0.3130E+00
0.4143E+04	0.3180E+02	0.5000E+01	-0.3000E+00
0.4149E+04	0.3180E+02	0.2913E+03	-0.2254E+00
0.4160E+04	0.3180E+02	0.9028E+02	0.1396E+00
0.4170E+04	0.3180E+02	0.2400E+02	0.3000E+00
0.4203E+04	0.3180E+02	0.4608E+03	-0.3308E+00
0.4221E+04	0.3180E+02	0.6891E+02	0.5839E+00
0.4241E+04	0.3180E+02	0.6000E+01	-0.5800E+01
0.4260E+04	0.3180E+02	0.8000E+01	0.7839E+01
0.4271E+04	0.3180E+02	0.1593E+03	0.1927E+00
0.4280E+04	0.3180E+02	0.3100E+02	-0.3000E+00
0.4288E+04	0.3180E+02	0.3230E+03	0.1519E+00
0.4315E+04	0.3180E+02	0.3500E+02	-0.2983E+00
0.4329E+04	0.3180E+02	0.3189E+03	-0.3957E-01
0.4338E+04	0.3180E+02	0.7500E+01	0.3000E+00

240-Pu Resonance Parameters (Contd.)

Energy (eV)	Width		
	Capture (meV)	Neutron (meV)	Fission (meV)
0.4363E+04	0.3180E+02	0.2000E+02	0.5865E+00
0.4376E+04	0.3180E+02	0.8200E+02	0.0000E+00
0.4386E+04	0.3180E+02	0.3200E+02	-0.6364E+00
0.4398E+04	0.3180E+02	0.7800E+02	-0.1036E+01
0.4415E+04	0.3180E+02	0.5000E+02	0.1295E+02
0.4422E+04	0.3180E+02	0.6100E+02	0.3074E+00
0.4433E+04	0.3180E+02	0.4700E+02	0.3054E+01
0.4447E+04	0.3180E+02	0.1800E+02	-0.3600E+00
0.4459E+04	0.3180E+02	0.1028E+03	0.6744E+00
0.4473E+04	0.3180E+02	0.2500E+02	-0.3000E+00
0.4491E+04	0.3180E+02	0.2000E+02	-0.3000E+00
0.4502E+04	0.3180E+02	0.2000E+02	0.3000E+00
0.4517E+04	0.3180E+02	0.1000E+02	-0.1879E+01
0.4538E+04	0.3180E+02	0.2600E+02	0.3000E+00
0.4560E+04	0.3180E+02	0.2000E+02	0.3000E+00
0.4570E+04	0.3180E+02	0.2352E+03	-0.3596E+00
0.4588E+04	0.3180E+02	0.5498E+03	-0.3089E+00
0.4599E+04	0.3180E+02	0.7539E+02	-0.3602E+00
0.4614E+04	0.3180E+02	0.2645E+03	-0.5836E+00
0.4646E+04	0.3180E+02	0.1521E+03	0.5416E+00
0.4664E+04	0.3180E+02	0.8000E+01	-0.3000E+00
0.4687E+04	0.3180E+02	0.2000E+02	0.3649E+01
0.4713E+04	0.3180E+02	0.5600E+02	0.5000E+00
0.4721E+04	0.3180E+02	0.5100E+03	-0.1300E+00
0.4745E+04	0.3180E+02	0.2525E+03	0.3000E+00

240-Pu Resonance Parameters (Contd.)

Energy (eV)	Width		
	Capture (meV)	Neutron (meV)	Fission (meV)
0.4755E+04	0.3180E+02	0.5469E+02	-0.1979E+01
0.4769E+04	0.3180E+02	0.3726E+02	0.1593E+01
0.4778E+04	0.3180E+02	0.3421E+02	0.1420E+01
0.4792E+04	0.3180E+02	0.1370E+03	0.1571E+01
0.4800E+04	0.3180E+02	0.2000E+02	-0.5000E+00
0.4812E+04	0.3180E+02	0.1812E+03	0.2535E+00
0.4823E+04	0.3180E+02	0.6338E+02	0.3645E+01
0.4843E+04	0.3180E+02	0.1802E+02	0.5382E+01
0.4868E+04	0.3180E+02	0.1300E+02	-0.7874E+01
0.4894E+04	0.3180E+02	0.6281E+02	-0.2464E+01
0.4911E+04	0.3180E+02	0.1500E+02	-0.4910E+02
0.4933E+04	0.3180E+02	0.2000E+02	0.2014E+02
0.4948E+04	0.3180E+02	0.5168E+02	-0.1990E+02
0.4958E+04	0.3180E+02	0.3197E+03	0.1229E+01
0.4969E+04	0.3180E+02	0.1537E+03	0.1298E+01
0.4975E+04	0.3180E+02	0.7500E+02	-0.5000E+00
0.4995E+04	0.3180E+02	0.9560E+02	-0.6463E+01
0.5035E+04	0.3180E+02	0.1500E+02	0.4094E+01
0.5047E+04	0.3180E+02	0.1000E+02	-0.2952E+01
0.5073E+04	0.3180E+02	0.5655E+03	-0.7727E+01
0.5097E+04	0.3180E+02	0.3601E+02	0.3349E+01
0.5112E+04	0.3180E+02	0.8608E+02	0.3853E+02
0.5120E+04	0.3180E+02	0.1950E+02	-0.5000E+00
0.5134E+04	0.3180E+02	0.4365E+02	-0.1832E+02
0.5148E+04	0.3180E+02	0.5000E+02	0.0000E+00

240-Pu Resonance Parameters (Contd.)

Energy (eV)	Width		
	Capture (meV)	Neutron (meV)	Fission (meV)
0.5162E+04	0.3180E+02	0.4000E+02	0.4020E+01
0.5175E+04	0.3180E+02	0.8000E+01	-0.5000E+01
0.5194E+04	0.3180E+02	0.3455E+03	0.9789E+00
0.5216E+04	0.3180E+02	0.1624E+03	-0.1691E+01
0.5235E+04	0.3180E+02	0.2400E+02	0.5610E+01
0.5248E+04	0.3180E+02	0.5226E+03	-0.5312E+01
0.5278E+04	0.3180E+02	0.1439E+03	0.2732E+02
0.5286E+04	0.3180E+02	0.5300E+02	0.5032E+00
0.5299E+04	0.3180E+02	0.2826E+03	0.1728E+02
0.5334E+04	0.3180E+02	0.1784E+03	-0.3188E+02
0.5351E+04	0.3180E+02	0.1503E+03	0.6624E+01
0.5356E+04	0.3180E+02	0.3600E+02	-0.4887E+00
0.5367E+04	0.3180E+02	0.6973E+02	-0.1930E+01
0.5380E+04	0.3180E+02	0.8000E+01	0.5073E+00
0.5393E+04	0.3180E+02	0.8465E+02	0.4246E+00
0.5418E+04	0.3180E+02	0.2642E+03	0.2029E+00
0.5440E+04	0.3180E+02	0.1200E+02	-0.6335E+01
0.5456E+04	0.3180E+02	0.8000E+01	-0.5041E+00
0.5465E+04	0.3180E+02	0.4971E+02	0.8704E+01
0.5483E+04	0.3180E+02	0.8875E+02	-0.4205E+01
0.5498E+04	0.3180E+02	0.9920E+02	0.5036E+00
0.5511E+04	0.3180E+02	0.3581E+03	-0.7952E+00
0.5522E+04	0.3180E+02	0.1752E+03	0.1587E+01
0.5531E+04	0.3180E+02	0.1600E+02	-0.5096E+00
0.5545E+04	0.3180E+02	0.5510E+03	-0.3428E+00

240-Pu Resonance Parameters (Contd.)

Energy (eV)	Width		
	Capture (meV)	Neutron (meV)	Fission (meV)
0.5551E+04	0.3180E+02	0.1211E+03	-0.4720E+00
0.5564E+04	0.3180E+02	0.1500E+02	0.4807E+00
0.5574E+04	0.3180E+02	0.7899E+03	0.1185E+00
0.5592E+04	0.3180E+02	0.1962E+03	0.2982E+00
0.5600E+04	0.3180E+02	0.1408E+03	-0.2462E+00
0.5615E+04	0.3180E+02	0.6200E+02	0.6971E+00
0.5629E+04	0.3180E+02	0.2000E+02	-0.4887E+00
0.5644E+04	0.3180E+02	0.5500E+02	0.4972E+00
0.5667E+04	0.3180E+02	0.4500E+02	-0.5064E+00
0.5681E+04	0.3180E+02	0.1054E+03	-0.8942E+00
0.5692E+04	0.3180E+02	0.9100E+02	0.0000E+00

INTERNAL DISTRIBUTION

1-2. Laboratory Records Dept.
3. Laboratory Records, ORNL-RC
4. Central Research Library
5. B. L. Broadhead
6-11. H. Derrien
12. F. C. Difilippo
13. C. Y. Fu
14. N. M. Greene
15. K. Guber
16. J. A. Harvey
17. C. M. Hopper
18. D. T. Ingersoll
19. P. E. Koehler
20. M. A. Kuliasha
21. D. C. Larson
22-26. N. M. Larson
27-31. L. C. Leal
32. C. V. Parks
33. R. W. Roussin
34. C. H. Shappert
35. M. S. Smith
36. R. R. Spencer
37. R. M. Westfall
38. J. E. White
39. R. Q. Wright
40. RSICC

EXTERNAL DISTRIBUTION

41. P. Blaise, DER/SPRC/LEPH, Batiment 230, Centre d'Etudes de CADARACHE, 13108 Saint Paul-lez-Durance, France
42. R. Block, Rensselaer Polytechnic Institute, Troy, NY 12180-3590
43-47. O. Bouland, DER/SPRC/LEPH, Batiment 230, Centre d'Etudes de CADARACHE, 13108 Saint Paul-lez-Durance, France
48. D. Cabrilla, U.S. Department of Energy, EM-66, Clover Leaf, Room 1199, 19901 Germantown Road, Germantown, MD 20874-1290
49. D. E. Carlson, Reactor and Plant System Branch, Division of System Research, Office of Nuclear Regulatory Research, U.S. Nuclear Regulatory Commission, MS T-10 G6, RM T-10, I7, Washington, DC 20555-0001
50. F. Corvi, Central Bureau for Nuclear Measurements, Steenweg op Retie, 2240 Geel, Belgium
51. R. L. Dintaman, U.S. Department of Energy, DP-13, Washington, DC 20585
52. C. Dunford, Bldg 197D, National Nuclear Data Center, Brookhaven National Laboratory, Upton, NY 11973
53. J. R. Felty, U. S. Department of Energy, DP-311, Washington DC 20585
54. P. Finck, Argonne National Laboratory, Reactor Analysis Division, Bldg 208, Argonne, IL 60439
55. C. M. Frankle, NIS-6, MS J562, Los Alamos National Laboratory, Los Alamos, NM 87545
56. S. C. Frankle, X-TM, MS B226, Los Alamos National Laboratory, Los Alamos, NM 87545
57. F. Froehner, Kernforschungszentrum Karlsruhe, Institut fuer Neutronenphysik und Reacktortechnik, Postfach 336 40, D-76021 Karlsruhe, Germany
58. W. Furman, Frank Laboratory of Neutron Physics, JINR, Dubna, Russia
59. S. Ganesan, Head, Nuclear Data Section, Indira Gandhi Centra for Atomic Research, Kalpakkam 603 102, Tamilnadu, India
60. H. Gruppelaar, Netherlands Energy Research Foundation ECN, Westerduinweg 3, P. O. Box 1, NL 1755 ZG Petten, Netherlands
61. F. Gunsing, Centre D'Etudes De Saclay, F-Saclay - 91191 GIF-SUR-YVETTE Cedex, France
62. G. M. Hale, T-2, MS B243, Los Alamos National Laboratory, Los Alamos, NM 87545

63. A. Hasagawa, Nuclear Data Center, Japan Atomic Energy Research Institute, Tokai-mura, Naka-gun, Ibaraki-ken 319-11, Japan
64. R. N. Hwang, Argonne National Laboratory, Reactor Analysis Division, Bldg 208, Argonne, IL 60439
65. R. P. Jacqmin, DER/SPRC/LEPH, Batiment 230, Centre d'Etudes de CADARACHE, 13108 Saint Paul-lez-Durance, France
66. N. Janeva, Bulgarian Academy of Sciences, 72, Boul, Tzarigradsko shosse, Sofia 1784, Bulgaria
67. L. Lambros, 08 E23, U.S. Nuclear Regulatory Commission, 11555 Rockville Pike, Rockville, MD 20852-2746
68. R. Little, X-TM, MS B226, Los Alamos National Laboratory, Los Alamos, NM 87545
69. C. Lubitz, Knolls Atomic Power Laboratory, P. O. Box 1072, Schnectady, NY 12301
70. R. E. MacFarlane,T-2, MS B243, Los Alamos National Laboratory, Los Alamos, NM 87545
71. C. Mounier, CEN Saclay, DMT/SERMA/LENR, 91191 Gif Sur Yvette Cedex, France
72. M. C. Moxon, 3 Hyde Copse, Marcham, Abingdon, Oxfordshire, England
73. D. Muir, IAEA Nuclear Data Section, Wagramerstr. 5, P. O. Box 100, A-1400 Wien, Austria
74. C. W. Nilson, Office of Nuclear Regulatory Research, U.S. Nuclear Regulatory Commission, Mail Stop TWFN 9-F-33, Washington, DC 20555
75. C. Nordborg, OECD/NEA, Le Seine St-Germain 12, Boulevard Iles, 92130 Issy-les-Moulineaux, France
76. C.Raepsaet, CEN Saclay, DMT/SERMA/LEPP, 91191 Gif Sur Yvette Cedex, France
77. M. Salvatores, DRN/P, Batiment 707, C. E. CADARACHE, 13108 Saint Paul-lez-Durance, France
78. E. Sartori, OECD/NEA, Le Seine St-Germain 12, Boulevard Iles, 92130 Issy-les-Moulineaux, France
79. O. A. Shcherbakov, Petersburg Nuclear Physics Institute, 188 350 Gatchina, Leningrad district, Russia
80. R. Shelley, Central Bureau for Nuclear Measurements, Steenweg op Retie, 2240 Geel, Belgium
81. K. Shibata, Nuclear Data Center, Japan Atomic Energy Research Institute, Tokai-mura, Naka-gun, Ibaraki-ken 319-11, Japan
82. D. L. Smith, TD-207-DB116, Argonne National Laboratory, Argonne, IL 60544
83. H. Takano, Nuclear Data Center, Japan Atomic Energy Research Institute, Tokai-mura, Ibaraki-ken 319-11, Japan
84. H. Weigmann, Central Bureau for Nuclear Measurements, Steenweg op Retie, 2240 Geel, Belgium
85. C. Werner, Renssalaer Polytechnic Institute, Troy, NY 12180-3590
86. R. White, Lawrence Livermore National Laboratory, P. O. Box 808, Livermore, CA 94550
87. M. Williams, Nuclear Science Center, Louisiana State University, Baton Rouge, LA 70803